Open access • Journal Article • DOI:10.1111/1462-2920.14092

The ecological genetics of Pseudomonas syringae from kiwifruit leaves

Christina Straub, Elena Colombi, Li Li, Hongwen Huang ...+5 more authors

Institutions: Massey University, Chinese Academy of Sciences, ParisTech, Max Planck Society

Published on: 01 Jun 2018 - Environmental Microbiology (Blackwell Science)

Topics: Pseudomonas syringae

The ecological genetics of *Pseudomonas syringae* from kiwifruit leaves

Christina Straub[1], Elena Colombi[1], Li Li[2], Hongwen Huang[2,3], Matthew D. Templeton[4], Honour C. McCann[1*], Paul B. Rainey[1, 5, 6*]

[1] New Zealand Institute for Advanced Study, Massey University, Auckland, New Zealand. [2] Key Laboratory of Plant Germplasm Enhancement and Specialty Agriculture, Wuhan Botanical Garden, Chinese Academy of Sciences, Wuhan, China. [3]Key Laboratory of Plant Resources Conservation and Sustainable Utilization, South China Botanical Garden, Chinese Academy of Sciences, Guangzhou, China. [4]Plant and Food Research, Auckland, New Zealand. [5]Max Planck Institute for Evolutionary Biology, Department of Microbial Population Biology, Plön, Germany. [6]École Supérieure de Physique et de Chimie Industrielles de la Ville de Paris (ESPCI Paris Tech), Laboratoire de Génétique de l'Evolution, Paris, France. * Joint senior authors

CORRESPONDENCE: Christina Straub, New Zealand Institute for Advanced Study, Massey University, Private Bag 102 904, Auckland 0745, New Zealand. Telephone: +64 9 4140800 ext 43811. e-mail: c.straub@massey.ac.nz

RUNNING TITLE (50 CHARACTERS)

Ecological genetics of *Pseudomonas syringae*

ORIGINALITY-SIGNIFICANT STATEMENT

Bacterial pathogen populations are often studied with little consideration of co-occurring microbes and yet interactions between pathogens and commensals can

affect both population structure and disease progression. A fine-scale sampling of commensals present on kiwifruit leaves during an outbreak of bleeding canker disease caused by *P. syringae* pv. *actinidiae* reveals a clonal population structure. A new clade of non-pathogenic *P. syringae* (PG3a) appears to be associated with kiwifruit on a global scale. The presence of PG3a on kiwifruit has significant effects on the outcome of infection by *P. syringae* pv. *actinidiae*. This emphasises the value of studying the effect of co-occurring bacteria on pathogen-plant interactions.

SUMMARY

Interactions between commensal microbes and invading pathogens are understudied, despite their likely effects on pathogen population structure and infection processes. We describe the population structure and genetic diversity of a broad range of co-occurring *Pseudomonas syringae* isolated from infected and uninfected kiwifruit during an outbreak of bleeding canker disease caused by *P. syringae* pv. *actinidiae* (*Psa*) in New Zealand. Overall population structure was clonal and affected by ecological factors including infection status and cultivar. Most isolates are members of a new clade in phylogroup 3 (PG3a), also present on kiwifruit leaves in China and Japan. Stability of the polymorphism between pathogenic *Psa* and commensal *P. syringae* PG3a isolated from the same leaf was tested using reciprocal invasion from rare assays *in vitro* and *in planta*. *P. syringae* G33C (PG3a) inhibited *Psa* NZ54, while the presence of *Psa* NZ54 enhanced the growth of *P. syringae* G33C. This effect could not be attributed to virulence activity encoded by the Type 3 secretion system of *Psa*. Together our data contribute toward

43 the development of an ecological perspective on the genetic structure of pathogen
44 populations.

45 **INTRODUCTION**

46 Kiwifruit (*Actinidia* spp.) cultivation is challenged by outbreaks of the
47 bacterial pathogen *Pseudomonas syringae* pv. *actinidiae (Psa)* – the causative agent
48 of bleeding canker disease. The latest outbreak was first reported in Italy in 2008
49 (Balestra *et al.*, 2008) before spreading rapidly through most kiwifruit growing
50 regions of the world (Abelleira *et al.*, 2011; Everett *et al.*, 2011; Koh *et al.*, 2012;
51 Zhao *et al.*, 2013; Sawada, 2015), arriving in New Zealand in 2010 (Everett *et al.*,
52 2011).

53 As a pathogen, *Psa* faces the challenge of colonising diverse environments
54 before proliferating in the apoplast and vascular tissues. Colonisation of leaf surfaces
55 prior to invasion is a key infection stage (Wilson and Lindow, 1994; Wilson *et al.*,
56 1999; Monier and Lindow, 2003; Pfeilmeier *et al.*, 2016). On the leaf surface *Psa* is
57 likely to encounter and interact with a diverse range of plant-colonising bacteria
58 (Hirano and Upper, 2000; Lindow and Brandl, 2003). Physical proximity increases the
59 likelihood of competitive interactions affecting disease outcomes (Lindow and
60 Brandl, 2003; Hibbing *et al.*, 2010) and increases the probability of horizontal gene
61 transfer (Sawada *et al.*, 1999; Polz *et al.*, 2013; Colombi *et al.*, 2017).

62 The local context and the scale of sampling bacterial populations is particularly
63 important, as it can have an impact on genetic structure (Istock *et al.*, 1992; Souza *et*
64 *al.*, 1992; Haubold and Rainey, 1996; Spratt and Maiden, 1999). A study by Istock *et*

al. (1992) made a particularly persuasive case by showing that sampling *Bacillus subtilis* at the local level (instead of pooled collections) contradicted the common view of its clonal population structure. Similar lessons regarding the scale of sampling have come from studying *P. syringae* populations with a range of structures reported depending upon whether or not environmental isolates are included (Sarkar and Guttman, 2004; Monteil *et al.*, 2013).

Bacterial interactions are context-dependent, ranging from synergistic to antagonistic, and may have both local and global effects on the plant host (Stubbendieck *et al.*, 2016). Antagonistic or competitive interactions between microbes may be direct or indirect, resulting in the inhibition of growth or even killing (Lindow, 1986; Völksch and May, 2001; Berlec, 2012; Hockett *et al.*, 2015; Nakahara *et al.,* 2016). Synergistic interactions occur when multiple types cooperate to cause disease (Singer, 2010; Lamichhane and Venturi, 2015). For example, *P. savastanoi* pv. *savastanoi,* causative agent of olive knot disease, interacts with non-pathogenic endophytes *Erwinia sp.* and *Pantoea sp.* in cankers, enhancing the severity of disease (Marchi *et al.*, 2006; Moretti *et al.*, 2011; Buonaurio *et al.*, 2015). Synergistic interactions can also be exploitative: bacteria lacking virulence factors can reap benefits from co-existing pathogenic isolates (Young, 1974; Hirano *et al.*, 1999; Macho *et al.*, 2007; Rufián *et al.*, 2017).

P. syringae is a common member of the phyllosphere (defined as the aerial part of a plant (Vorholt, 2012)) and engages in both commensal and pathogenic interactions with plants (Hirano and Upper, 2000; Mohr *et al.*, 2008). The diversity and population structure of *P. syringae* has been investigated using both multilocus

sequence typing (MLST) and genome sequence analysis of pathogenic isolates collected from diseased plants (Sarkar and Guttman, 2004; Hwang *et al.*, 2005; Baltrus *et al.*, 2011; McCann *et al.*, 2013, 2017; Fujikawa and Sawada, 2016; Nowell *et al.*, 2016). Studies have also explored the structure of *P. syringae* populations from environmental reservoirs beyond standard host plants (Morris *et al.*, 2008; Monteil *et al.*, 2013, 2014, 2016). However, the genetic structure of specific pathovar populations from the phyllosphere of specific host plants have rarely been studied in the context of co-occurring *P. syringae* types.

Here we describe the population structure of the *P. syringae* species complex inhabiting the kiwifruit phyllosphere during an outbreak of bleeding canker disease in New Zealand. Using an MLST scheme, we reveal a largely clonal population structure, but show that genetic diversity is significantly affected by ecological factors such as infection status and cultivar. We identified members of four *P. syringae* phylogroups (PG1, PG2, PG3 and PG5) and recovered a new monophyletic clade within PG3 (PG3a) that is associated with kiwifruit in different kiwifruit-growing regions of the world. Investigations into the ecological interactions between a representative of this new clade and *Psa* show that PG3a restricts *Psa* proliferation, while *Psa* facilitates growth of PG3a.

RESULTS

Phyllosphere diversity of *Pseudomonas syringae*

Four housekeeping genes (*gapA*, *gyrB*, *gltA*, *rpoD*) were sequenced for each of 148 *P. syringae* isolated from two varieties of kiwifruit ('Hayward' and 'Hort16A')

in both uninfected and *Psa*-infected orchards. Rarefaction analysis indicates saturation of the sampling effort (Figure S1). The infected 'Hayward' orchard displayed the highest α-diversity (D=0.904), while the uninfected 'Hort16A' orchard displayed the least α-diversity (D=0.737). There was low evenness (ED) among all sampling sites (0.136 to 0.290). Similarly, the four different sampling sites shared few species (Sørensen's index of dissimilarity = 0.847).

Multilocus sequence typing

45 unique sequence types (ST) were discovered among the 148 sequenced strains. All STs were novel, except for ST904 (*Psa*), and not described in the Plant Associated and Environmental Microbes Database (PAMDB). For a more global analysis, *P. syringae* allelic profiles were sourced from PAMDB and NCBI (accessions listed in Table S2), along with *P. syringae* isolated from kiwifruit in Japan (NCBI) , NZ and the US (Visnovsky *et al.* 2016).

Infected orchards (both 'Hayward' and 'Hort16A') harboured the highest number of unique STs, sharing only three STs between them (Figure S2). No STs were present in all four orchards, but two STs were found in three orchards (ST1 and ST3). From the perspective of clonal complexes (CC), the predominant ST (predicted founder) was present along with several SLVs (single locus variants). Two clonal complexes (CC) (21 strains), 5 doubletons (32 strains) and 28 singletons (95 strains) were identified (Figure S3). CC1 and CC2 are comprised of 11 and 10 strains, respectively. ST904 (*Psa*, 15/148) and ST1 (PG3, 24/148) made up 25% of the sample (Figure S3). Strikingly, ST3 (PG3a) was isolated from three out of four orchards and was also sampled from uninfected gold (*A. chinensis* var. *chinensis*) and green (*A.*

133 *chinensis* var. *deliciosa*) kiwifruit in NZ (2010) (Visnovsky *et al.*, 2016) and Japan
134 (2015), respectively (Figure 1). ST16 was also recovered from uninfected kiwifruit
135 leaves in NZ in both 1991 and 2013. Other Japanese kiwifruit STs group closely with
136 *P. syringae* originating from kiwifruit in NZ.

137 **Sequence diversity**

138 The total concatenated alignment length was 2010 bp with no insertions or
139 deletions detected for either of the four loci. The number of alleles ranged from 25
140 (*gapA*) to 35 (*rpoD*) (Table 1). There were a total of 412 polymorphic sites, ranging
141 from 80 (16.81%, *gapA*) to 145 (28.6%, *gyrB*). The nucleotide diversity index π and
142 Watterson's θ were highly consistent among loci, varying from 0.040 to 0.055 and
143 0.024 to 0.041 respectively. The average GC content of 57.99% is similar to that
144 found in other *P. syringae* studies (59- 61%). The pairwise genetic difference within
145 phylogroups (PGs) was not greater than 2.7%, whereas among PGs the variability
146 ranged from 6-11% (Table 2), consistent with previous accounts of genetic variability
147 for *P. syringae* (Sarkar and Guttman, 2004; Morris *et al.*, 2010; Berge *et al.*, 2014).

148 **Genetic diversity varies by host cultivar and infection status**

149 To test whether genetic diversity was influenced by the presence of
150 ecological structure, multivariate analyses (PERMANOVA) were performed. A highly
151 significant difference in genetic diversity was observed among sampled orchards
152 (Pseudo-F = 5.99, $P < 0.0001$); with pairwise Permanova tests revealing that the
153 uninfected green orchard differed significantly from every other orchard ($P<0.003$).
154 The cultivar ('Hayward' vs. 'Hort16A') (Pseudo-F = 5.62, $P<0.001$) and infection status

of an orchard (Pseudo-F = 11.72, *P* <0.001) also had a significant effect on genetic diversity, whereas no temporal effect was found (Pseudo-F = 1.10, *P* >0.34). When testing the nested effect of all three factors, only the infection status (Pseudo-F = 6.42, *P* <0.01) had a significant impact on genetic diversity (Table S3).

Recombination among *P. syringae*

Intragenic recombination rates (ρ) ranged from 0.012 (*rpoD*) to 0.038 (*gyrB*) and 0.006 for the concatenated dataset. The ratio ε (recombination rate/mutation rate) ranged from 0.187 (concatenated*)* to 0.931 (*gyrB*) suggesting that any single nucleotide polymorphism is up to five times more likely to have arisen from a mutation than recombination (Table 3).

Clustering sequences by PG revealed no evidence of recombination within PG1 and PG5 (ρ=0), however for these phylogroups the sample size was low. There was evidence of recombination in PG3, more specifically for *gltA* (ε=1.18) and *rpoD* (ε=4.07), whereas in PG2 recombination was evident in *rpoD* (ε=1.734) alone. Recombination was neither affected by the host cultivar or infection status (Table S4). The analysis was repeated with the inclusion of non-redundant global strains. Overall, intergenic recombination rates were low among PGs, ranging from 0.005 to 0.012 for the concatenated dataset (Table S5). In order to pinpoint any effects of recombination on phylogenetic reconstruction, single gene trees were constructed and compared. Tree topologies were significantly different from each other and from the concatenated dataset (SH test, *P*<0.05) (Figure S4).

A kiwifruit-associated clade of *P. syringae*

Maximum likelihood trees built using the concatenated alignment of unique STs revealed that nearly all NZ *P. syringae* kiwifruit isolates fell within four PGs: PG1 (13%), PG2 (29%) and PG3 (56%), with only a few isolates falling into PG5 (2%, Figure 2). Surprisingly, within PG3 all NZ kiwifruit-associated isolates grouped within a new clade of PG3, hereafter referred to as PG3a. The uninfected orchards showed a higher number of PG3a isolates compared to infected orchards, although no influence of infection status was reflected in the number of unique sequence types (Table S1). We also found that two strains isolated from kiwifruit in NZ in 2010 and 2011 (Visnovsky *et al.*, 2016) belong to this subclade.

This discovery led us to question whether the PG3a subclade might be prevalent on kiwifruit vines in other countries. To this end we interrogated an unpublished set of *gltA* sequences from *P. syringae* strains collected from kiwifruit leaves in China (sampling as described in McCann *et al.* (2017), GenBank accession numbers: MG674624 – MG674645). A phylogenetic tree based on *gltA* for NZ, Japanese and Chinese kiwifruit isolates revealed that isolates obtained from Chinese kiwifruit also clustered within PG3a (Figure 3). Interestingly, included in this group is isolate 47L9, which was collected from tea leaves (*Camellia* sp.) growing in a former kiwifruit orchard in China. No other *P. syringae* strain from the PAMDB database grouped with PG3a, suggesting PG3a is persistently associated with kiwifruit on a global scale.

196 **Ecological interactions between PG3a and PG1**

197 To assess whether kiwifruit-associated PG3a strains are stably maintained
198 with *Psa* (PG1), co-inoculation experiments were performed *in vitro* and *in planta*.
199 Two isolates sampled from the same leaf were chosen for these experiments: *P.*
200 *syringae* G33C (ST1, PG3a) and *Psa* NZ54 (ST904, PG1).

201 **In vitro *dynamics***

202 *Psa* NZ54 and *P. syringae* G33C showed similar growth dynamics when grown
203 individually *in vitro* (Figure 4). However, when co-inoculated in liquid King's B (KB)
204 media at an equal starting ratio, *Psa* NZ54 growth was significantly reduced (up to
205 100-fold) at 24 h (P <0.001, paired t-tests). This effect was amplified in shaken liquid
206 minimal M9 medium, which better approximates nutrient poor conditions in the leaf
207 compared to KB medium (Hernández-Morales *et al.*, 2009): *Psa* NZ54 population
208 density collapsed by 20 h in shaken M9 media (relative fitness -12.1 ±0.09, Figure 4).

209 In order to establish whether the instability of the interaction was influenced
210 by the ratio of founder cells, we investigated whether *P. syringae* G33C could invade
211 from rare initial frequency. A strain is able to invade from rare when it increases
212 relative to its founding density. *P. syringae* G33C successfully invaded from rare after
213 only 24 h in both rich KB and minimal M9 media (10:1 *Psa NZ54* : *P. syringae* G33C)
214 and reached a similar population size as when cultured on its own in M9 (Figure 5A).
215 Conversely, *Psa* NZ54 also invaded *P. syringae* G33C from rare (*1:10 Psa* NZ54 : *P.*
216 *syringae* G33C), though it established a 100-fold reduced population size of 10^5 - 10^6
217 cfu ml^{-1} compared to growth alone. The population collapse of *Psa* NZ54 in shaken

M9, as observed for the 1:1 competition experiments, was once again observed (Figure 5B). The striking suppression of *Psa* NZ54 by *P. syringae* G33C was unambiguously repeated across three experiments. *P. syringae* G33C outcompetes *Psa* NZ54, though both isolates can invade from rare *in vitro* (with the exception of *Psa* NZ54 in shaken M9), which suggests that in a controlled environment the polymorphism is stable.

In planta *dynamics*

In planta experiments were performed on two gold cultivars, 'Hort16A' and 'SunGold', to determine whether *Psa* NZ54 and *P. syringae* G33C also form a stable polymorphism on kiwifruit leaves. *P. syringae* G33C established an epiphytic and endophytic population size in both cultivars (Figure 6) and did not produce any visible symptoms in 'Hort16A' and 'SunGold' (Figure S5, Figure S6). *Psa* NZ54 attained a population size at least 10,000-fold greater than *P. syringae* G33C in both hosts. However, endophytic and epiphytic growth were reduced 10-fold in 'SunGold' compared to 'Hort16A' (P <0.05, Mann-Whitney U test). Plants inoculated with *Psa* NZ54 developed the first leaf spots at 4 dpi and exhibited severe symptoms at 7 dpi in the more susceptible 'Hort16A', whereas in 'SunGold' leaves displayed only minor symptoms at 7 dpi.

In 1:1 competition experiments non-pathogenic *P. syringae* G33C maintained a stable population size. The presence of *Psa* NZ54 had a highly significant positive effect on the growth of *P. syringae* G33C in both plant hosts (Figure 6A&B). *P. syringae* G33C established up to 1000-fold higher epiphytic population densities in 'Hort16A' (P <0.01, paired t-tests) and 10-fold higher epiphytic and endophytic

241 population densities in 'SunGold' plants (P <0.05, paired t-test) compared to its
242 individual growth. Co-inoculated *Psa* NZ54 exhibited a significant reduction (P <0.05,
243 paired t-test) in epiphytic and endophytic growth on 'Hort16A' in the presence of *P.*
244 *syringae* G33C, but only in the early stages of the experiment. On 'SunGold' the
245 diminished growth of *Psa* NZ54 was more pronounced, with a 100-fold decrease for
246 the endophytic population at 7 dpi (P <0.05, paired t-test, Figure 6B). Co-inoculated
247 'Hort16A' plants exhibited a notable delay in symptom onset compared to singly
248 inoculated plants (Figure S5), whereas there was no difference for 'SunGold' (Figure
249 S6). The increased fitness of *Psa* NZ54 relative to *P. syringae* G33C in 'Hort16A'
250 competition experiments was reflected in the relative fitness parameters (0.7± 0.1*
251 for epiphytic and 4.9± 0.8* for endophytic, * P <0.05, t-test), whereas in 'SunGold'
252 plants *P. syringae* G33C performed better in the epiphytic environment (-1.6 ± 0.2;
253 4.7 ± 0.1* for endophytic growth).

254 To assess whether the heightened growth of *P. syringae* G33C in the
255 presence of *Psa* NZ54 was due to the virulence activity of the pathogen elicited by
256 the Type 3 Secretion System (T3SS), the competition experiment was performed
257 using a T3SS deficient mutant (*Psa* NZ13 Δ*hrcC*). Epiphytic growth of *P. syringae*
258 G33C on 'SunGold' remained elevated when co-inoculated with *Psa* NZ13 Δ*hrcC*,
259 indicating the virulence activity encoded by the T3SS was not responsible for the
260 advantage conferred to the non-pathogenic strain (P <0.05, paired t-test, Figure 6C).

261 A rarity threshold for *P. syringae* G33C determines the ability to establish a stable
262 population *in planta*. Upon co-inoculation in a 100:1 (*Psa* NZ54 : *P. syringae* G33C)
263 ratio on 'Hort16A', *P. syringae* G33C was able to invade from rare over the first 4

264 days, but was then excluded by *Psa* NZ54 (Figure 7B). An initial increase in growth of
265 *P. syringae* G33C from 0 dpi to 4 dpi was followed by a population collapse at 7 dpi
266 with no endophytic growth detected and minimal epiphytic growth in environments
267 dominated by *Psa* NZ54. Conversely, *Psa* NZ54 grew to the same population size in
268 the presence of *P. syringae* G33C, as when inoculated individually (P >0.1, paired t-
269 tests).

270 In the reciprocal experiment (1:100 *Psa* NZ54 : *P. syringae* G33C), *Psa* NZ54
271 successfully invaded from rare in both the endophytic and epiphytic environment,
272 although the rate of invasion was reduced on the leaf surface . However, both epi-
273 and endophytic population sizes were significantly reduced compared to single
274 inoculations (P <0.01, paired t-tests) (Figure 7). Despite the growing population of
275 *Psa* NZ54, *P. syringae* G33C maintained the same epiphytic population size as when
276 inoculated individually (P >0.2, paired t-tests). The endophytic population size of *P.*
277 *syringae* G33C increased (P <0.01, 7dpi, paired t-test), which mirrored the results
278 from the 1:1 competition experiments, where the presence of *Psa* NZ54 also had a
279 positive effect on growth of *P. syringae* G33C.

280 In order to establish whether there was an advantage to being an early
281 colonist, a time-stagger experiment was performed to see whether immigration
282 history influences the interaction (Fukami *et al.*, 2007). 'Hort16A' plants were pre-
283 inoculated with either of the two strains and followed by a subsequent inoculation
284 of the other strain after three days. Early colonization provided no advantage to *Psa*
285 NZ54 (Figure 8A), as *P. syringae* G33C maintained and established a stable
286 population by 7 dpi and exhibited no significant difference in growth compared to

individual growth (P >0.3, paired t-tests). Reducing the secondary inoculation density resulted in a reduced initial population size at 3 and 7 dpi for *P. syringae* G33C (P <0.05, paired t-tests), but by 10 dpi the level was the same as when the two strains were grown individually (Figure S7C).

When *P. syringae* G33C was the first colonist (Figure 8B) *Psa* NZ54 grew to the same population size by 7 dpi as compared to individually inoculated plants (P >0.5, paired t-tests). The growth of *Psa* NZ54 was initially lower compared to individual growth when inoculated at a lower density (P <0.05, paired t-tests), but this difference was no longer evident for the epiphytic population by 10 dpi (Figure S7B).

DISCUSSION

Studies of pathogen populations rarely take into consideration co-occurring commensal types and yet such types are likely to be important contributors to population structure and infection progress (Lindow and Brandl, 2003; Demba Diallo *et al.*, 2012; Bartoli *et al.*, 2015; Buonaurio *et al.*, 2015; Rufián *et al.*, 2017). Here, with focus on *P. syringae*, we have combined traditional population genetic approaches with experiments designed to investigate interactions among members of an ecologically cohesive population. The most significant findings include (i) a clonal population structure for commensal kiwifruit *P. syringae* (ii) strong association of genetic diversity with ecological factors, (iii) discovery of a new clade of kiwifruit-associated kiwifruit *P. syringae* within PG3 (PG3a) (Figure 2, Figure 3), (iv) complex

interactions between the pathogenic *Psa* isolate and PG3a with evidence of a stable polymorphism under some *in vitro* conditions, but not *in planta* (Figure 4, Figure 6).

Overall, we found that *P. syringae* from kiwifruit display a clonal population structure, comprised of two clonal complexes and a small number of abundant STs. This is in accordance with earlier reports of clonal population structure for *P. syringae*, despite focus on pathogenic isolates which tend to undergo clonal expansion upon host specialisation (Sarkar and Guttman, 2004). Homologous recombination events are few and limited to within phylogroups for *P. syringae*, which is also supported by well-defined phylogenetic clades (Baltrus *et al.*, 2011; Bull *et al.*, 2011; Berge *et al.*, 2014; Nowell *et al.*, 2016). A more fine-scale analysis of a collection of *Pseudomonas viridiflava* (now *P. syringae* PG7 and PG8 (Bartoli *et al.*, 2014; Berge *et al.*, 2014)) isolated from *Arabidopsis thaliana* suggests that recombination at the phylogroup level is primarily within-clade rather than between clade (Goss *et al.*, 2005). Apart from the occurrence of recombination at the local scale, evidence of recombination has also been shown between crop strains and environmental isolates (Monteil *et al.*, 2013).

Genetic diversity varied according to ecological factors, most strikingly for *P. syringae* collected from infected orchards, where genetic diversity was highest. This may reflect effects of *Psa* on the kiwifruit immune response, which may facilitate migration of leaf colonists into the apoplast and vascular tissues and thus allow access to water and nutrients. Such effects have been reported for infection of potatoes by *Pectobacterium atrosepticum* (Kõiv *et al.*, 2015) and herbivore-damaged bitter cress leaves (*Cardamine cordifolia*) (Humphrey *et al.*, 2014), where in both

331 instances *Pseudomonas* population densities and diversity increased following plant
332 damage.

333 We observed differences in *P. syringae* genetic diversity that appear to be
334 attributable to differences in plant genotypes. Host species and cultivar identity is
335 known to significantly affect the composition of phyllosphere bacterial communities
336 (Adams and Kloepper, 2002; Van Overbeek and Van Elsas, 2008; Whipps *et al.*, 2008;
337 Bodenhausen *et al.*, 2014; Laforest-Lapointe *et al.*, 2016; Wagner *et al.*, 2016).
338 Differences in phyllosphere *P. syringae* diversity may also be influenced by
339 environmental factors (such as humidity, nutrient availability or UV radiation) and
340 orchard management practices. Different fertilizer and spray regimes (copper,
341 antibiotics, Actigard™ and biological agents) are employed by growers to prevent or
342 manage *Psa* infection throughout the growing season
343 (http://www.kvh.org.nz/vdb/document/99346). These practices may have selected
344 for copper and streptomycin resistance in *Psa* and kiwifruit epiphytes in NZ and
345 elsewhere (Han *et al.*, 2003; Colombi *et al.*, 2017; Petriccione *et al.*, 2017).

346 Strains grouping with four major phylogroups (PG1, PG2, PG3, PG5) were
347 recovered. This level of diversity in a cultivated environment is not surprising (Goss
348 *et al.*, 2005; Bull *et al.*, 2011; Kniskern *et al.*, 2011; Beiki *et al.*, 2016; Hall *et al.*,
349 2016). Two clades of endophytic *P. syringae* pv. *syringae* were recovered from
350 symptomatic grapevines in Australia with pathogenic and non-pathogenic isolates
351 clustering together (Hall *et al.*, 2016). Samples obtained from citrus orchards
352 suffering from citrus blast caused by *P. syringae* pv. *syringae* revealed isolates
353 associated with PG2, PG7 and an unknown clade (Beiki *et al.*, 2016). Two distinct and

354 highly divergent subclades of *Pseudomonas viridiflava* (*P. syringae* PG7) were
355 recovered from a global sampling of wild *A. thaliana* (Goss *et al.*, 2005).

356 The newly recognised PG3a subclade of *P. syringae* appear to colonise
357 kiwifruit leaves not only in NZ (dating back to 2010 (Visnovsky *et al.*, 2016)), but also
358 in other kiwifruit growing regions of the world, including Japan and China. Data from
359 leaf samples indicate that PG3a is not displaced by *Psa*, but the total number of
360 PG3a isolates collected is reduced in infected orchards. Interestingly the diversity of
361 PG3a does not seem to be affected by infection status. Strains clustering with PG3a
362 formed the majority (>50%) of kiwifruit isolates, and these have not yet been
363 isolated from any other plant hosts recorded in PAMDB, with the exception of isolate
364 47L9, collected from tea leaves (*Camellia* sp.) growing in a former kiwifruit orchard.
365 This indicates that PG3a forms a persistent association with kiwifruit plants – an
366 observation that is further supported by the repeated isolation of PG3a from
367 kiwifruit across large geographic distances, suggests that PG3a may have been
368 coevolving with its host for some time. PG3a is thus also likely to be disseminated
369 with the exchange of plant material (such as pollen or plant cuttings) between
370 kiwifruit growing countries. The prevalence of PG3a in other kiwifruit growing
371 countries (e.g. Korea, France or Italy) is at present unknown. The preferential
372 occurrence of PG3 with woody hosts (Bartoli *et al.*, 2015; Nowell *et al.*, 2016) could
373 explain the particular grouping of the kiwifruit resident clade within PG3. A similarly
374 intriguing signal of host association was found in a collection of *P. syringae* isolates
375 from *A. thaliana*, where PG2 representatives dominated (Kniskern *et al.*, 2011;
376 Karasov *et al.*, 2017). Distinct lineages of non-pathogenic isolates have also been

described for other plant pathogens such as *Xanthomonas arboricola,* where non-pathogenic strains are distant relatives of pathogenic lineages, despite being isolated from the same host (Essakhi *et al.*, 2015; Triplett *et al.*, 2015).

The kiwifruit commensal *P. syringae* G33C (representative of the PG3a subclade) successfully colonized the leaf surface and apoplast of kiwifruit without production of visible disease symptoms. This is reflected in the population size, which was reduced by 4-logs compared to pathogenic population size of *Psa* at 3 dpi. Similar population sizes have been reported for *P. syringae* pv. *phaseolicola*, which grows to a four-log higher population size on its host plant *Phaseolus vulgaris* compared to a non-pathogenic isolate; a 4-log reduction was also observed in resistant vs susceptible hosts (Omer and Wood, 1969; Young, 1974). Similar observations have been made for other plant pathogens, for example non-pathogenic *Xanthomonas* sp. displays a 4-log reduced growth compared to the disease-causing *X. oryzae* pv. *oryzae* (Triplett *et al.*, 2015). Bacterial population density appears to be directly related to the production of disease symptoms, as was demonstrated for environmental *P. syringae* strains inoculated in kiwifruit, which grew to near pathogen population size levels, but induced symptoms of disease (Bartoli *et al.*, 2015).

When grown in competition with *Psa* NZ54, *P. syringae* G33C population size increased. Studies exploring the dynamics of mixed infections have demonstrated inoculum density-dependent effects on colonization (Young, 1974; Macho *et al.*, 2007). The ability of non-pathogenic *P. syringae* to colonize wider territories in the presence of a pathogenic strain was nicely demonstrated in a

confocal microscopy study (Rufián *et al.*, 2017). It is possible that *P. syringae* G33C benefits from the virulence activity of *Psa* NZ54. T3SS-dependent hitch-hiking effects have been observed for *P. syringae* pv. *syringae* (Hirano *et al.*, 1999), however the increase *in P.* syringae G33C growth persists even in the absence of a functional T3SS in the pathogenic *Psa* strain. Virulence activities not encoded by the T3SS, such as phytotoxin production, may be responsible for this outcome.

Epiphytic and *in vitro* growth of *Psa* NZ54 was significantly reduced when co-inoculated with *P. syringae* G33C. Similarly, *Psa* growth may be suppressed by co-inoculation with environmental isolates of *P. syringae* (Bartoli *et al.*, 2015). Epiphytes may suppress pathogen growth either as direct antagonists or indirectly via resource competition (Wilson and Lindow, 1994). The specific mechanism by which *P. syringae* G33C suppresses *Psa* remains undetermined. The *Psa* NZ54 population collapse in shaken M9 was delayed at 10:1 inoculation ratios, which suggests that this effect was most likely due to the accumulation of antimicrobial compounds produced by *P. syringae* G33C. Phytotoxin production is widespread among fluorescent pseudomonads with some toxins having antimicrobial activity that can be induced dependent on culture conditions (still vs. shaken) *in vitro* (Durbin, 1982; Bender *et al.*, 1999). Contact-dependant growth inhibition (CDI) via Type 5 and 6 secretion systems or bacteriocins may also mediate *P. syringae* interactions (Hayes *et al.*, 2010; Haapalainen *et al.*, 2012; Ruhe *et al.*, 2013; Hockett *et al.*, 2015).

Our in-depth localised sampling has revealed a global association of PG3a with kiwifruit. Additionally, we have shown that this clade of non-pathogenic *P. syringae* engage in complex interactions with pathogenic *Psa*. This highlights the

value of understanding genotypic diversity and ecological interactions among pathogens and non-pathogens in field settings. Clarifying how commensals persist in association with specific hosts over long periods without causing disease and the mechanism by which they modulate pathogen invasion and proliferation will contribute to a fuller understanding of plant-microbe interactions.

EXPERIMENTAL PROCEDURES

Plant tissue collection and bacterial isolation

The sampling scheme was designed to obtain strains from *Psa* infected and uninfected hosts, irrespective of disease stage (symptom development) or pathogenicity potential of the isolate. *P. syringae* was isolated from the leaf surfaces of two different cultivars of *Actinidia chinensis*: *A. chinensis* var. *chinensis* Hort16A (gold) and *A. chinensis* var. *deliciosa* Hayward (green), which vary in their susceptibility to *Psa*: 'Hort16A' is more susceptible than the green 'Hayward' (Ferrante and Scortichini, 2010; Cameron and Sarojini, 2014). One infected and one uninfected orchard of each variety was sampled by collecting three leaves from six separate vines along a diagonal path of ~400m (Table S1). Sampling occurred at three intervals during the growing season: spring (after bud break), summer and autumn (prior to harvest). Vine trunks and canes (secondary branches) were tagged to ensure resampling of the same spot. Some 'Hort16A' canes were removed during routine disease management; neighbouring canes on the same vine were then sampled and tagged. All uninfected Hayward vines were cut down prior to the last

444 sampling day so the adjoining block of Hayward was sampled instead. The location of
445 each sampled orchard is listed in Table S2.

446 Leaves were individually placed in 50 mL conical centrifuge tubes and washed
447 with 40 mL 10mM $MgSO_4$ buffer supplemented with 0.2 % Tween (Invitrogen, US) by
448 alternately shaking and vortexing at slow speed for 3 min. After removing the leaf,
449 the leaf wash was centrifuged at 4600 rpm for 10 min. The supernatant was
450 removed and the pellet was resuspended in 200 µL 10mM $MgSO_4$. 100 µL of the
451 resuspension was stored at -80°C and 100 µL was plated on *Pseudomonas* agar base
452 (Oxoid, UK) supplemented with 10 mg/L cetrimide, 10 mg/L fucidin and 50 mg/L
453 cephalosporin (CFC supplement, Oxoid, UK). For each leaf two isolates exhibiting *P.*
454 *syringae* colony morphology (round, creamy white) were selected randomly from
455 the plate and restreaked, then used to inoculate liquid overnight cultures for storage
456 at -80˚C. Isolates were tested for the absence of cytochrome *C* oxidase using
457 Bactident Oxidase strips (Merck KgaA, Germany), characteristic of *P. syringae*. A total
458 of 148 *P. syringae* isolates were obtained from the four orchards (Table S1).

459 **PCR amplification & sequencing**

460 A lysate was prepared for each isolate by resuspending a colony in 100 µL ddH_20 and
461 lysing the cells at 96°C for 10 min. Strains were sequenced using the Hwang *et al.*
462 (2005) MLST scheme for four housekeeping genes *gapA*, *gyrB*, *gltA (=cts)* and *rpoD*
463 (reverse). Due to amplification problems, the forward primer for *rpoD* from Sarkar
464 and Guttman (2004) was used. PCR amplification was performed with a BIO-RAD
465 T100 Thermal Cycler following an adapted protocol of Hwang et al. (2005): a total
466 reaction volume of 50 µl with a final concentration of 1x PCR buffer (Invitrogen, US),

1 µM for each primer, 0.2 mM dNTP's (Bioline, UK), 1 U Taq Polymerase (Invitrogen, US), 1 µl lysed bacterial cells, 2% DMSO (Sigma-Aldrich, US) and 1.5 mM $MgCl_2$. Initial denaturation was at 94°C for 2 min, followed by 30 cycles of amplification with denaturation at 94°C for 30 s, annealing at 63°C for 30 s and elongation at 72°C for 1 min. Final elongation was for 3 min at 72°C. Samples were purified using the Exo-CIP method and sequenced by Macrogen Inc (South Korea). Sequence analysis was performed with Geneious v7.1.7 (Kearse *et al.*, 2012). Sequences were trimmed to the same length (476 bp *gap1*, 507 bp *gyrB*, 529 bp *gltA*, 498 bp *rpoD*) and concatenated (2010 bp) (GenBank accession numbers: *gapA* MG642149 - MG642296; *gyrB* MG642297 - MG642444; *gltA* MG642445 - MG642592; *rpoD* MG642593 - MG642740).

Population genetics

Sequence diversity indices

A rarefaction analysis was performed using MOTHUR v.1.34.4 by subsampling using 1,000 iterations (Schloss *et al.*, 2009). Pairwise genetic distances between isolates were calculated and sequences assigned to Operational Taxonomic Units (OTUs) based on the corresponding average pairwise genetic distance of each group.

Simpson's index of diversity (D) and evenness (ED) (α-diversity) and Sørensen's index of dissimilarity (β-diversity) were calculated using the *vegan* package (Oksanen *et al.*, 2016) in R v3.3.1 (R.Core.Team, 2016). Simpson's D was converted to the effective number of species (D_c) in order to account for the non-linear properties of Simpson's index of diversity (Jost, 2006).

Multilocus Sequence Typing

Sequence types (STs) sharing three out of four alleles (SLV, single locus variants) were grouped using eBURST v3 (bootstrapped with 1,000,000 resamplings) (Feil *et al.*, 2004; Spratt *et al.*, 2004). A Minimum Spanning Tree providing an overview of triple locus variants was constructed using Phyloviz v2.0 (Francisco *et al.*, 2012).

165 non-redundant ST profiles of *P. syringae* strains were downloaded from the Plant Associated and Environmental Microbes Database (PAMDB, http://genome.ppws.vt.edu/cgi-bin/MLST/home.pl) (Almeida *et al.*, 2010). *P. syringae* sequences isolated recently from kiwifruit and air in Japan (NCBI) and kiwifruit isolates from NZ, France and the United States (Visnovsky *et al.*, 2016) were also included. A reduced set of 37 *P. syringae* isolates representing the different monophyletic groups of *P. syringae*, as well as the Japanese kiwifruit strains and the US, France and NZ kiwifruit isolates from previous years were used to provide better resolution in the phylogenies displayed in Figure 2, Figure 3 and Figure S4.

Sequence diversity and recombination

START2 (v0.9.0 beta) was employed to calculate parameters of genetic diversity, number of alleles and polymorphic sites, GC content and the ratio of non-synonymous to synonymous substitutions (d_N/d_S ratio) (Jolley *et al.*, 2001). The number of mutations and amino acid changes and nucleotide diversity parameter π were calculated with DnaSP v. 5.10.1 (Rozas and Rozas, 1995). Jmodeltest 2.1.7 (Guindon and Gascuel, 2003; Darriba *et al.*, 2012) was used with default parameter

511 settings to find the best-fitting evolutionary model. Pairwise genetic variability
512 among and between phylogroups was calculated using MEGA7 (Kumar *et al.*, 2016).

513 To test whether genetic diversity varied by sampling location, time of sampling,
514 orchard infection status and/or cultivar, a permutational multivariate analysis of
515 variance (PERMANOVA) (Anderson, 2001; McArdle and Anderson, 2001) was
516 performed using PRIMER v 6.1.12 (PRIMER-E Ltd., Plymouth, UK, PERMANOVA+ add-
517 on v. 1.0.2.). Pairwise distances among unique STs were used as input and tests were
518 run with 9999 permutations. Any effects due to unequal sample size were taken into
519 account using the Type III SS (sum of squares) option.

520 LDHAT v2.2a (Auton and McVean, 2007) was used to estimate the rate of
521 mutation (Watterson's θ) and recombination (ρ) using the composite likelihood
522 method of Hudson (Hudson, 2001) with an adaption to finite-site models. Only
523 polymorphic sites with two alleles were included and the frequency cut-off for
524 missing data was set to 0.2.

525 *Phylogenetic reconstruction*

526 Trees were built using single representatives of each unique ST from this
527 study to improve readability of the tree. MrBayes v.3.2 (Ronquist *et al.*, 2012) was
528 used to construct Bayesian trees, using the best-fitting evolutionary model
529 (jModeltest) for individual genes and the concatenated alignment. Single gene trees
530 (Figure S4) were constructed with TREEPUZZLE (Schmidt *et al.*, 2002) and Dnaml
531 (PHYLIP v3.695, Felsenstein 1989) was used to test for congruence between single
532 trees (SH-test) using default parameters, providing Maximum Likelihood trees as
533 input and a random number seed of 333.

Strains and culture conditions

A list of all bacterial strains used in this study can be found in Table S2. *Pseudomonas* strains were cultured in King's B or minimal M9 media at 28˚C and *E. coli* was cultured in Luria Bertani medium at 37˚C. Liquid overnight cultures were inoculated from single colonies and shaken at 250 rpm for 16 hrs. The antibiotics kanamycin (kan) and nitrofurantoin (nf) were used at a concentration of 50 µg/ml. Kanamycin resistant *Psa* NZ54 and *Psa* NZ13 Δ*hrcC* were employed in all *in vitro* and *in planta* experiments. Both *Psa* strains belong to the same pandemic clade of *Psa* (biovar 3), and differ in three SNPs across the core genome as defined in McCann *et al.* (2017).

Mutant development

Psa NZ13Δ*hrcC* was constructed by in-frame deletion of *hrcC* via marker exchange mutagenesis. Knockout construct was generated by overlap extension PCR (Ho *et al.*, 1989) using the primers listed in Table S6. DNA was amplified from *Psa* NZ13 with Phusion® High-Fidelity DNA polymerase. The deletion construct was inserted into pK18mobsacB (Schäfer *et al.*, 1994). The recombinant vector was transferred into *Psa* NZ13 via triparental mating, using as helper *E. coli* DH5α strain containing pRK2013. Mutants were selected by plating on KB kanamycin (50 µg/mL) and subsequently on KB containing 5% sucrose. Mutants were screened by PCR using external primers (Table S6) and the deletion was then confirmed by sequencing.

Triparental matings were performed to introduce a kanamycin resistant Tn*5* transposon into *Psa* NZ54 and *Psa* NZ13 Δ*hrcC*. *E. coli* S17-1 Tn*5hah Sgid1* (donor)

(Zhang *et al.*, 2015), *E. coli pRK2013* (helper) (Ditta *et al.*, 1980) and *Psa* NZ54 or *Psa* NZ13 Δ*hrcC* (recipient) were grown in shaken liquid media overnight. 200 µl of donor and helper and 2mL of recipient were individually washed, pelleted and combined in 30 µl 10 mM $MgCl_2$. The mixture was plated on a pre-warmed LB agar plate and incubated at 28˚C for 24 hrs. The cells were scraped off and resuspended in 1 mL 10 mM $MgCl_2$ and plated on KB plates supplemented with kanamycin and nitrofurantoin. Bacterial growth was compared to the wild type recipient in both KB and M9 media to ensure marker introduction did not result in a loss of fitness.

Competition assays

The two isolates (*P. syringae* G33C and *Psa* NZ54) used for competition assays were isolated from the same leaf in a *Psa* infected orchard, reflecting co-occurrence of the strains in nature.

In vitro competition assays

Competition experiments were performed *in vitro* using rich (King's B) and minimal (M9) media in a shaken and static environment. Competition experiments were performed in 1:1, 1:10 and 10:1 ratios for each of the four assay conditions. Liquid overnight cultures of each strain in KB were established from single colony inoculations. 30 mL vials with 4 mL of the appropriate media were inoculated with each strain, adjusted to a founding density of either $5x10^6$ cfu ml^{-1} (OD_{600} 0.006) or $4x10^4$ cfu ml^{-1} (OD_{600} 0.0004). Control vials were inoculated with a single strain, adjusted to $5x10^6$ cfu ml^{-1}. Cultures were incubated at 28˚C and grown over a period of 72 hrs, either still or shaken at 250rpm. Bacterial density was calculated at 0, 24,

48 and 72 hrs by plating dilutions on KB kan and M9 agar plates to distinguish between competing strains. The experiment was performed using three replicates and repeated three times.

In planta competition and pathogenicity assays

Epiphytic and endophytic growth of *Psa* NZ54, *Psa* NZ13 Δ*hrcC* and *P. syringae* G33C was evaluated on 4-week old kiwifruit plantlets using single and mixed-culture inoculation. Clonally propagated *A. chinensis* var. *chinensis* 'Hort16A' and 'SunGold' were grown for a minimum of one month in a Conviron CMP6010 growth cabinet at 21˚C with a 14/10 hr light/dark cycle and 70% humidity. Bacterial strains were incubated for two days at 28˚C on KB plates, after which they were resuspended in 10 mM $MgSO_4$ buffer. Mixed inoculum (1:1, 1:100 and 100:1) was prepared in 50 mL 10 mM $MgSO_4$ buffer and 0.002% Silwet-70 (surfactant), with strains adjusted to $8x10^7$ cfu ml^{-1} (OD_{600} 0.1) or $8x10^5$ cfu ml^{-1} (OD_{600} 0.001). Single strain plant inoculations were also performed using an initial $8x10^7$ cfu ml^{-1} (OD_{600} 0.1).

Plants were inoculated by submerging leaves in the inoculum for 5 s and allowing to air-dry. Plants were returned to the growth cabinet and watered every second day. Bacterial density was assessed at either 0, 2, 4, 7 and 10 days post inoculation (dpi) or 0, 3, and 7 dpi (Δ*hrcC* competition experiments). Epiphytic growth was assessed by placing inoculated leaves in separate sterile plastic bags with 35 mL 10 mM $MgSO_4$ buffer and shaking manually for 3 minutes. The leaf wash was centrifuged at 4600 rpm for 3 min and the supernatant discarded. Bacteria were

resuspended in 200 µl buffer and serial dilutions plated on M9 and KB+kan agar plates.

Endophytic growth was assessed by removing one $1cm^2$ leaf disk per plant (including the midrib), surface sterilizing in 70% EtOH for 30 sec, drying and homogenising for 1 minute in a 1.5 mL Eppendorf tube containing 200 µl buffer and two metal beads with the TissueLyser II (QIAGEN). The plant homogenate was serially diluted and plated on M9 and KB+kan agar plates. All experiments were performed in duplicate, with at least 4 replicates per experiment.

Statistical analysis

A Student's *t*-test was used to verify the statistical difference where applicable. For non-normally distributed data with unequal variance, the Mann Whitney U test was performed.

The fitness of each strain in the competition experiments is expressed as the Malthusian parameter (Lenski *et al.*, 1991). The Malthusian parameter was calculated as $M = (ln(N1_{f1}/N1_i))/(ln(N2_f/N2_i))$, where $N1_i$ is initial number of cfu of strain 1 at 0h and $N1_f$ cfu after 24 hrs (*in vitro*) or 2/3 dpi (*in planta,* 'Hort16A'/'SunGold').

BIOSECURITY AND APPROVAL

All worked was performed in approved facilities and in accord with APP201675, APP201730, APP202231.

ACKNOWLEDGEMENTS

We want to particularly thank kiwifruit growers David French, Rex Reed and Bruce and Fiona Aitken for granting access to their orchards. The work conducted was supported by the New Zealand Ministry for Business, Innovation and Employment (C11X1205). Christina Straub was supported through a PhD scholarship from the New Zealand Institute for Advanced Studies (NZIAS) and Plant & Food Research.

REFERENCES

Abelleira, A., López, M.M., Peñalver, J., Aguín, O., Mansilla, J.P., Picoaga, A., and García, M.J. (2011) First report of bacterial canker of kiwifruit Caused by Pseudomonas syringae pv. actinidiae in Spain. *Plant Dis.* **95**: 1583.

Adams, P.D. and Kloepper, J.W. (2002) Effect of host genotype on indigenous bacterial endophytes of cotton (Gossypium hirsutum L.). *Plant Soil* **240**: 181–189.

Almeida, N.F., Yan, S., Cai, R., Clarke, C.R., Morris, C.E., Schaad, N.W., et al. (2010) PAMDB, a multilocus sequence typing and analysis database and website for plant-associated microbes. *Phytopathology* **100**: 208–215.

Anderson, M.J. (2001) A new method for non parametric multivariate analysis of variance. *Austral Ecol.* **26**: 32–46.

Auton, A. and McVean, G. (2007) Recombination rate estimation in the presence of hotspots. *Genome Res.* **17**: 1219–1227.

Balestra, G.M., Mazzaglia, A., Spinelli, R., Graziani, S., Quattrucci, A., and Rossetti, A. (2008) Cancro batterico su Actinidia chinensis. *L'informatore Agrar.* **38**: 75–76.

Baltrus, D.A., Nishimura, M.T., Romanchuk, A., Chang, J.H., Mukhtar, M.S., Cherkis, K., et al. (2011) Dynamic evolution of pathogenicity revealed by sequencing and comparative genomics of 19 Pseudomonas syringae isolates. *PLoS Pathog.* **7**: e1002132.

Bartoli, C., Berge, O., Monteil, C.L., Guilbaud, C., Balestra, G.M., Varvaro, L., et al. (2014) The Pseudomonas viridiflava phylogroups in the P. syringae species complex are characterized by genetic variability and phenotypic plasticity of pathogenicity-related traits. *Environ. Microbiol.* **16**: 2301–2315.

Bartoli, C., Lamichhane, J.R., Berge, O., Guilbaud, C., Varvaro, L., Balestra, G.M., et al. (2015) A framework to gauge the epidemic potential of plant pathogens in environmental reservoirs: the example of kiwifruit canker. *Mol. Plant Pathol.* **16**: 137–49.

Beiki, F., Busquets, A., Gomila, M., Rahimian, H., Lalucat, J., and García-Valdés, E. (2016) New Pseudomonas spp. are pathogenic to citrus. *PLoS One* **11**: e0148796.

Bender, C.L., Alarcon-Chaidez, F., Gross, D.C., Alarcón-Chaidez, F., and Gross, D.C. (1999) Pseudomonas syringae phytotoxins: Mode of action, regulation, and biosynthesis by peptide and polyketide synthetases. *Microbiol. Mol. Biol. Rev.* **63**: 266–292.

Berge, O., Monteil, C.L., Bartoli, C., Chandeysson, C., Guilbaud, C., Sands, D.C., and Morris, C.E. (2014) A user's guide to a data base of the diversity of Pseudomonas syringae and its application to classifying strains in this phylogenetic complex. *PLoS One* **9**: e105547.

Berlec, A. (2012) Novel techniques and findings in the study of plant microbiota: Search for plant probiotics. *Plant Sci.* **193–194**: 96–102.

Bodenhausen, N., Bortfeld-Miller, M., Ackermann, M., and Vorholt, J.A. (2014) A Synthetic Community Approach Reveals Plant Genotypes Affecting the Phyllosphere Microbiota. *PLoS Genet.* **10**: e1004283.

Bull, C.T., Clarke, C.R., Cai, R., Vinatzer, B.A., Jardini, T.M., and Koike, S.T. (2011) Multilocus sequence typing of Pseudomonas syringae sensu lato confirms previously described genomospecies and permits rapid identification of P. syringae pv. coriandricola and P. syringae pv. apii causing bacterial leaf spot on parsley. *Phytopathology* **101**: 847–858.

Buonaurio, R., Moretti, C., da Silva, D.P., Cortese, C., Ramos, C., and Venturi, V. (2015) The olive knot disease as a model to study the role of interspecies bacterial communities in plant disease. *Front. Plant Sci.* **6**: 1–12.

Cameron, A. and Sarojini, V. (2014) Pseudomonas syringae pv. actinidiae: chemical control, resistance mechanisms and possible alternatives. *Plant Pathol.* **63**:.

Colombi, E., Straub, C., Künzel, S., Templeton, M.D., McCann, H.C., and Rainey, P.B. (2017) Evolution of copper resistance in the kiwifruit pathogen Pseudomonas syringae pv. actinidiae through acquisition of integrative conjugative elements and plasmids. *Environ. Microbiol.* **19**: 819–832.

Darriba, D., Taboada, G.L., Doallo, R., and Posada, D. (2012) jModelTest 2: more models, new heuristics and parallel computing. *Nat. Methods* **9**: 772–772.

Demba Diallo, M., Monteil, C.L., Vinatzer, B.A., Clarke, C.R., Glaux, C., Guilbaud, C., et al. (2012) Pseudomonas syringae naturally lacking the canonical type III secretion system are ubiquitous in nonagricultural habitats, are phylogenetically diverse and can be pathogenic. *ISME J.* **6**: 1325–1335.

Ditta, G., Stanfield, S., Corbin, D., and Helinski, D.R. (1980) Broad host range DNA cloning system for gram-negative bacteria: construction of a gene bank of Rhizobium meliloti. *Proc. Natl. Acad. Sci.* **77**: 7347–7351.

Durbin, R.D. (1982) Toxins and Pathogenesis. In, Mount,M.S. and Lacy,G.H. (eds), *Phytopathogenic Prokaryotes Vol 1*. Academic Press, pp. 423–439.

Essakhi, S., Cesbron, S., Fischer-Le Saux, M., Bonneau, S., Jacques, M.A., and Manceau, C. (2015) Phylogenetic and variable-number tandem-repeat analyses identify nonpathogenic Xanthomonas arboricola lineages lacking the canonical type III secretion system. *Appl. Environ. Microbiol.* **81**: 5395–5410.

Everett, K.R., Taylor, R.K., Romberg, M.K., Rees-George, J., Fullerton, R.A., Vanneste, J.L., and Manning, M.A. (2011) First report of Pseudomonas syringae pv. actinidiae causing kiwifruit bacterial canker in New Zealand. *Australas. Plant Dis. Notes* **6**: 67–71.

Feil, E.J., Li, B.C., Aanensen, D.M., Hanage, W.P., and Spratt, B.G. (2004) eBURST:

704 inferring patterns of evolutionary descent among clusters of related bacterial
705 genotypes from Multilocus Sequence Typing Data. *J. Bacteriol.* **186**: 1518–1530.
706 Felsenstein, J. (1989) Phylip: phylogeny inference package (version 3.2). *Cladistics* **5**:
707 164–166.
708 Ferrante, P. and Scortichini, M. (2010) Molecular and phenotypic features of
709 Pseudomonas syringae pv. actinidiae isolated during recent epidemics of
710 bacterial canker on yellow kiwifruit (Actinidia chinensis) in central Italy. *Plant*
711 *Pathol.* **59**: 954–962.
712 Francisco, A.P., Vaz, C., Monteiro, P.T., Melo-Cristino, J., Ramirez, M., and Carriço,
713 J.A. (2012) PHYLOViZ: phylogenetic inference and data visualization for
714 sequence based typing methods. *BMC Bioinformatics* **13**: 87.
715 Fujikawa, T. and Sawada, H. (2016) Genome analysis of the kiwifruit canker pathogen
716 Pseudomonas syringae pv. actinidiae biovar 5. *Sci. Rep.* **6**:.
717 Fukami, T., Beaumont, H.J.E., Zhang, X.-X., and Rainey, P.B. (2007) Immigration
718 history controls diversification in experimental adaptive radiation. *Nature* **446**:
719 436–439.
720 Goss, E.M., Kreitman, M., and Bergelson, J. (2005) Genetic diversity, recombination
721 and cryptic clades in Pseudomonas viridiflava infecting natural populations of
722 Arabidopsis thaliana. *Genetics* **169**: 21–35.
723 Guindon, S. and Gascuel, O. (2003) A simple, fast, and accurate algorithm to estimate
724 large phylogenies by maximum likelihood. *Syst. Biol.* **52**: 696–704.
725 Haapalainen, M., Mosorin, H., Dorati, F., Wu, R.F., Roine, E., Taira, S., et al. (2012)
726 Hcp2, a secreted protein of the phytopathogen Pseudomonas syringae pv.
727 tomato DC3000, is required for fitness for competition against bacteria and
728 yeasts. *J. Bacteriol.* **194**: 4810–4822.
729 Hall, S.J., Dry, I.B., Blanchard, C.L., and Whitelaw-Weckert, M.A. (2016) Phylogenetic
730 relationships of Pseudomonas syringae pv. syringae isolates associated with
731 bacterial iInflorescence rot in grapevine. *Plant Dis.* **100**: 607–616.
732 Han, H.S., Nam, H.Y., Koh, Y.J., Hur, J.-S., and Jung, J.S. (2003) Molecular bases of
733 high-level streptomycin resistance in Pseudomonas marginalis and
734 Pseudomonas syringae pv. actinidiae. *J. Microbiol.* **41**: 16–21.
735 Haubold, B. and Rainey, P.B. (1996) Genetic and ecotypic structure of a fluorescent
736 Pseudomonas population. *Mol. Ecol.* **5**: 747–761.
737 Hayes, C.S., Aoki, S.K., and Low, D.A. (2010) Bacterial contact-dependent delivery
738 systems. *Annu. Rev. Genet.* **44**: 71–90.
739 Hernández-Morales, A., De la Torre-Zavala, S., Ibarra-Laclette, E., Hernández-Flores,
740 J., Jofre-Garfias, A., Martínez-Antonio, A., and Álvarez-Morales, A. (2009)
741 Transcriptional profile of Pseudomonas syringae pv. phaseolicola NPS3121 in
742 response to tissue extracts from a susceptible Phaseolus vulgaris L. cultivar.
743 *BMC Microbiol.* **9**: 257.
744 Hibbing, M.E., Fuqua, C., Parsek, M.R., and Peterson, S.B. (2010) Bacterial
745 competition: surviving and thriving in the microbial jungle. *Nat. Rev. Microbiol.*
746 **8**: 15–25.
747 Hirano, S.S., Charkowski, A.O., Collmer, A., Willis, D.K., and Upper, C.D. (1999) Role of
748 the Hrp type III protein secretion system in growth of Pseudomonas syringae
749 pv. syringae B728a on host plants in the field. *Proc. Natl. Acad. Sci.* **96**: 9851–
750 9856.

751 Hirano, S.S. and Upper, C.D. (2000) Bacteria in the leaf ecosystem with emphasis on
752 Pseudomonas syringae - a pathogen, ice nucleus, and epiphyte. *Microbiol. Mol.*
753 *Biol. Rev.* **64**: 624–653.
754 Ho, S.N., Hunt, H.D., Horton, R.M., Pullen, J.K., and Pease, L.R. (1989) Site-directed
755 mutagenesis by overlap extension using the polymerase chain reaction. *Gene*
756 **77**: 51–59.
757 Hockett, K.L., Renner, T., and Baltrus, D.A. (2015) Independent co-option of a tailed
758 bacteriophage into a killing complex in Pseudomonas. *MBio* **6**: 1–11.
759 Hudson, R.R. (2001) Two-locus sampling distributions and their application. *Genetics*
760 **159**: 1805–1817.
761 Humphrey, P.T., Nguyen, T.T., Villalobos, M.M., and Whiteman, N.K. (2014) Diversity
762 and abundance of phyllosphere bacteria are linked to insect herbivory. *Mol.*
763 *Ecol.* **23**: 1497–1515.
764 Hwang, M.S.H., Morgan, R.L., Sarkar, S.F., Wang, P.W., and Guttman, D.S. (2005)
765 Phylogenetic characterization of virulence and resistance phenotypes of
766 Pseudomonas syringae. *Appl. Environ. Microbiol.* **71**: 5182–5191.
767 Istock, C.A., Duncan, K.E., Ferguson, N., and Zhou, X. (1992) Sexuality in a natural
768 population of bacteria - Bacillus subtilis challenges the clonal paradigm. *Mol.*
769 *Ecol.* **1**: 95–103.
770 Jolley, K.A., Feil, E.J., Chan, M.S., and Maiden, M.C. (2001) Sequence type analysis
771 and recombinational tests (START). *Bioinformatics* **17**: 1230–1231.
772 Jost, L. (2006) Entropy and diversity. *Oikos* **113**: 363–375.
773 Karasov, T.L., Barrett, L., Hershberg, R., and Bergelson, J. (2017) Similar levels of gene
774 content variation observed for Pseudomonas syringae populations extracted
775 from single and multiple host species. *PLoS One* **12**: 1–18.
776 Kearse, M., Moir, R., Wilson, A., Stones-Havas, S., Cheung, M., Sturrock, S., et al.
777 (2012) Geneious Basic: An integrated and extendable desktop software
778 platform for the organization and analysis of sequence data. *Bioinformatics* **28**:
779 1647–1649.
780 Kniskern, J.M., Barrett, L.G., and Bergelson, J. (2011) Maladaptation in wild
781 populations of the generalist plant pathogen Pseudomonas syringae. *Evolution*
782 *(N. Y).* **65**: 818–830.
783 Koh, Y.J., Kim, G.H., Koh, H.S., Lee, Y.S., Kim, S.C., and Jung, J.S. (2012) Occurrence of
784 a new type of Pseudomonas syringae pv. actinidiae strain of bacterial canker on
785 kiwifruit in Korea. *Plant Pathol.* **28**: 423–427.
786 Kõiv, V., Roosaare, M., Vedler, E., Ann Kivistik, P., Toppi, K., Schryer, D.W., et al.
787 (2015) Microbial population dynamics in response to Pectobacterium
788 atrosepticum infection in potato tubers. *Sci. Rep.* **5**: 11106.
789 Kumar, S., Stecher, G., and Tamura, K. (2016) MEGA7: Molecular Evolutionary
790 Genetics Analysis version 7.0 for bigger datasets. *Mol. Biol. Evol.* **33**: 1870–1874.
791 Laforest-Lapointe, I., Messier, C., Kembel, S.W., Lindow, S., Brandl, M., Herre, E., et
792 al. (2016) Host species identity, site and time drive temperate tree phyllosphere
793 bacterial community structure. *Microbiome* **4**: 27.
794 Lamichhane, J.R. and Venturi, V. (2015) Synergisms between microbial pathogens in
795 plant disease complexes: a growing trend. *Front. Plant Sci.* **6**: 385.
796 Lenski, R.E., Rose, M.R., Simpson, S.C., and Tadler, S.C. (1991) Long-term
797 experimental evolution in Escherichia coli . I . Adaptation and divergence during

2,000 generations. *Am. Nat.* **138**: 1315–1341.

Lindow, S.E. (1986) Construction of isogenic Ice strains of Pseudomonas syringae for evaluation of specificity of competition on leaf surfaces. *Perspect. Microb. Ecol. Slov. Soc. Microbiol. Ljubljana* 509–515.

Lindow, S.E. and Brandl, M.T. (2003) Microbiology of the phyllosphere. *Appl. Environ. Microbiol.* **69**: 1875–1883.

Macho, A.P., Zumaquero, A., Ortiz-Martín, I., and Beuzón, C.R. (2007) Competitive index in mixed infections: A sensitive and accurate assay for the genetic analysis of Pseudomonas syringae-plant interactions. *Mol. Plant Pathol.* **8**: 437–450.

Marchi, G., Sisto, A., Cimmino, A., Andolfi, A., Cipriani, M.G., Evidente, A., and Surico, G. (2006) Interaction between Pseudomonas savastanoi pv. savastanoi and Pantoea agglomerans in olive knots. *Plant Pathol.* **55**: 614–624.

McArdle, B.H. and Anderson, M.J. (2001) Fitting multivariate models to community data: a comment on distance-based redundancy analysis. *Ecology* **82**: 290–297.

McCann, H.C., Li, L.L., Liu, Y., Li, D., Pan, H., Zhong, C., et al. (2017) Origin and evolution of the kiwifruit canker pandemic. *Genome Biol. Evol.* **9**: 932–944.

McCann, H.C., Rikkerink, E.H.A., Bertels, F., Fiers, M., Lu, A., Rees-George, J., et al. (2013) Genomic analysis of the kiwifruit pathogen Pseudomonas syringae pv. actinidiae provides insight into the origins of an emergent plant disease. *PLoS Pathog.* **9**: e1003503.

Mohr, T.J., Liu, H., Yan, S., Morris, C.E., Castillo, J.A., Jelenska, J., and Vinatzer, B.A. (2008) Naturally occurring nonpathogenic isolates of the plant pathogen Pseudomonas syringae lack a type III secretion system and effector gene orthologues. *J. Bacteriol.* **190**: 2858–2870.

Monier, J.-M. and Lindow, S.E. (2003) Differential survival of solitary and aggregated bacterial cells promotes aggregate formation on leaf surfaces. *Proc. Natl. Acad. Sci.* **100**: 15977–15982.

Monteil, C.L., Cai, R., Liu, H., Mechan Llontop, M.E., Leman, S., Studholme, D.J., et al. (2013) Nonagricultural reservoirs contribute to emergence and evolution of Pseudomonas syringae crop pathogens. *New Phytol.* **199**: 800–811.

Monteil, C.L., Lafolie, F., Laurent, J., Clement, J.-C.C., Simler, R., Travi, Y., and Morris, C.E. (2014) Soil water flow is a source of the plant pathogen Pseudomonas syringae in subalpine headwaters. *Environ. Microbiol.* **16**: 2038–2052.

Monteil, C.L., Yahara, K., Studholme, D.J., Mageiros, L., Méric, G., Swingle, B., et al. (2016) Population-genomic insights into emergence, crop-adaptation, and dissemination of Pseudomonas syringae pathogens. *Microb. Genomics* **2**: 1–16.

Moretti, C., Hosni, T., Vandemeulebroecke, K., Brady, C., de Vos, P., Buonaurio, R., and Cleenwerck, I. (2011) Erwinia oleae sp. nov., isolated from olive knots caused by Pseudomonas savastanoi pv. savastanoi. *Int. J. Syst. Evol. Microbiol.* **61**: 2745–2752.

Morris, C.E., Sands, D.C., Vanneste, J.L., Montarry, J., Oakley, B., Guilbaud, C., and Glaux, C. (2010) Inferring the evolutionary history of the plant pathogen Pseudomonas syringae from its biogeography in headwaters of rivers in North America, Europe, and New Zealand. *MBio* **1**: e00107.

Morris, C.E., Sands, D.C., Vinatzer, B.A., Glaux, C., Guilbaud, C., Buffière, A., et al. (2008) The life history of the plant pathogen Pseudomonas syringae is linked to the water cycle. *ISME J.* **2**: 321–334.

Nakahara, H., Mori, T., Sadakari, N., Matsusaki, H., and Matsuzoe, N. (2016) Selection of effective non-pathogenic Ralstonia solanacearum as biocontrol agents against bacterial wilt in eggplant. *J. Plant Dis. Prot.* **123**: 119–124.

Nowell, R.W., Laue, B.E., Sharp, P.M., and Green, S. (2016) Comparative genomics reveals genes significantly associated with woody hosts in the plant pathogen Pseudomonas syringae. *Mol. Plant Pathol.* **17**: 1409–1424.

Oksanen, J., Blanchet, F.G., Friendly, M., Kindt, R., Legendre, P., Dan McGlinn, Peter R. Minchin, R.B.O., et al. (2016) vegan: Community Ecology Package.

Omer, M.E.H. and Wood, R.K.S. (1969) Growth of Pseudomonas phaseolicola in susceptible and in resistant bean plants. *Ann. Appl. Biol.* **63**: 103–116.

Van Overbeek, L. and Van Elsas, J.D. (2008) Effects of plant genotype and growth stage on the structure of bacterial communities associated with potato (Solanum tuberosum L.). *FEMS Microbiol. Ecol.* **64**: 283–296.

Petriccione, M., Zampella, L., Mastrobuoni, F., and Scortichini, M. (2017) Occurrence of copper-resistant Pseudomonas syringae pv. syringae strains isolated from rain and kiwifruit orchards also infected by P. s. pv. actinidiae. *Eur. J. Plant Pathol.* 1–16.

Pfeilmeier, S., Caly, D.L., and Malone, J.G. (2016) Bacterial pathogenesis of plants: future challenges from a microbial perspective: Challenges in Bacterial Molecular Plant Pathology. *Mol. Plant Pathol.* **17**: 1298–1313.

Polz, M.F., Alm, E.J., and Hanage, W.P. (2013) Horizontal gene transfer and the evolution of bacterial and archaeal population structure. *Trends Genet.* **29**: 170–175.

R.Core.Team (2016) R: A language and environment for statistical computing.

Ronquist, F., Teslenko, M., van der Mark, P., Ayres, D.L., Darling, A., Hohna, S., et al. (2012) MrBayes 3.2: Efficient Bayesian phylogenetic inference and model choice across a large model space. *Syst. Biol.* **61**: 539–542.

Rozas, J. and Rozas, R. (1995) DnaSP, DNA sequence polymorphism: an interactive program for estimating population genetics parameters from DNA sequence data. *CABIOS* **11**: 621–625.

Rufián, J.S., Macho, A.P., Corry, D.S., Mansfield, J., Arnold, D., and Beuzón, C.R. (2017) Confocal microscopy reveals in planta dynamic interactions between pathogenic, avirulent and non-pathogenic Pseudomonas syringae strains. *Mol. Plant Pathol.* DOI: 10.1111/mpp.12539.

Ruhe, Z.C., Low, D.A., and Hayes, C.S. (2013) Bacterial contact-dependent growth inhibition. *Trends Microbiol.* **21**: 230–237.

Sarkar, S.F. and Guttman, D.S. (2004) Evolution of the core genome of Pseudomonas syringae, a highly clonal, endemic plant pathogen. *Appl. Environ. Microbiol.* **70**: 1999–2012.

Sawada, H. (2015) Characterization of biovar 3 strains of Pseudomonas syringae pv. actinidiae isolated in Japan. *Japanese J. Phyopathology* **81**: 111–126.

Sawada, H.H., Suzuki, F.F., Matsuda, I.I., and Saitou, N.N. (1999) Phylogenetic analysis of Pseudomonas syringae pathovars suggests the horizontal gene transfer of argK and the evolutionary stability of hrp gene cluster. *J. Mol. Evol.* **49**: 627–644.

Schäfer, A., Tauch, A., Jäger, W., Kalinowski, J., Thierbach, G., and Pühler, A. (1994) Small mobilizable multi-purpose cloning vectors derived from the Escherichia

892 coli plasmids pK18 and pK19: selection of defined deletions in the chromosome
893 of Corynebacterium glutamicum. *Gene* **145**: 69–73.
894 Schloss, P.D., Westcott, S.L., Ryabin, T., Hall, J.R., Hartmann, M., Hollister, E.B., et al.
895 (2009) Introducing mothur: Open-source, platform-independent, community-
896 supported software for describing and comparing microbial communities. *Appl.*
897 *Environ. Microbiol.* **75**: 7537–7541.
898 Schmidt, H.A., Strimmer, K., Vingron, M., and von Haeseler, A. (2002) TREE-PUZZLE:
899 maximum likelihood phylogenetic analysis using quartets and parallel
900 computing. *Bioinformatics* **18**: 502–504.
901 Singer, M. (2010) Pathogen-pathogen interaction. *Virulence* **1**: 10–18.
902 Souza, V., Nguyen, T.T., Hudson, R.R., Piñero, D., and Lenski, R.E. (1992) Hierarchical
903 analysis of linkage disequilibrium in Rhizobium populations: evidence for sex?
904 *Proc. Natl. Acad. Sci. U. S. A.* **89**: 8389–93.
905 Spratt, B.G., Hanage, W.P., Li, B., Aanensen, D.M., and Feil, E.J. (2004) Displaying the
906 relatedness among isolates of bacterial species -- the eBURST approach. *FEMS*
907 *Microbiol. Lett.* **241**: 129–134.
908 Spratt, B.G. and Maiden, M.C.J. (1999) Bacterial population genetics, evolution and
909 epidemiology. *Philos. Trans. R. Soc. B Biol. Sci.* **354**: 701–710.
910 Stubbendieck, R.M., Vargas-Bautista, C., and Straight, P.D. (2016) Bacterial
911 communities: Interactions to scale. *Front. Microbiol.* **7**: 1234.
912 Triplett, L.R., Verdier, V., Campillo, T., Van Malderghem, C., Cleenwerck, I., Maes, M.,
913 et al. (2015) Characterization of a novel clade of Xanthomonas isolated from
914 rice leaves in Mali and proposal of Xanthomonas maliensis sp. nov. *Antonie van*
915 *Leeuwenhoek, Int. J. Gen. Mol. Microbiol.* **107**: 869–881.
916 Visnovsky, S.B., Fiers, M., Lu, A., Panda, P., Taylor, R., and Pitman, A.R. (2016) Draft
917 genome sequences of 18 strains of Pseudomonas isolated from kiwifruit plants
918 in New Zealand and overseas. *Genome Announc.* **4**: e00061-16.
919 Völksch, B. and May, R. (2001) Biological Control of Pseudomonas syringae pv.
920 glycinea by Epiphytic Bacteria under Field Conditions. *Microb. Ecol.* **41**: 132–
921 139.
922 Vorholt, J.A. (2012) Microbial life in the phyllosphere. *Nat. Rev. Microbiol.* **10**: 828–
923 840.
924 Wagner, M.R., Lundberg, D.S., del Rio, T.G., Tringe, S.G., Dangl, J.L., and Mitchell-
925 Olds, T. (2016) Host genotype and age shape the leaf and root microbiomes of a
926 wild perennial plant. *Nat. Commun.* **7**: 12151.
927 Whipps, J.M., Hand, P., Pink, D., and Bending, G.D. (2008) Phyllosphere microbiology
928 with special reference to diversity and plant genotype. *J. Appl. Microbiol.* **105**:
929 1744–1755.
930 Wilson, M., Hirano, S.S., and Lindow, S.E. (1999) Location and survival of leaf-
931 associated bacteria in relation to pathogenicity and potential for growth within
932 the leaf. *Appl. Environ. Microbiol.* **65**: 1435–1443.
933 Wilson, M. and Lindow, S.E. (1994) Coexistence among epiphytic bacterial
934 Populations mediated through nutritional resource partitioning. *Appl. Environ.*
935 *Microbiol.* **60**: 4468–4477.
936 Young, J.M. (1974) Development of bacterial populations in vivo in relation to plant
937 pathogenicity. *New Zeal. J. Agric. Res.* **17**: 105–113.
938 Zhang, X.X., Gauntlett, J.C., Oldenburg, D.G., Cook, G.M., and Rainey, P.B. (2015) Role

939 of the transporter-like sensor kinase CbrA in histidine uptake and signal
940 transduction. *J. Bacteriol.* **197**: 2867–2878.
941 Zhao, Z.B., Gao, X.N., Huang, Q.L., Huang, L.L., Qin, H.Q., and Kang, Z.S. (2013)
942 Identification and characerization of the causal agent of bacterial canker of
943 kiwifruit in the Shaanxi province of China. *J. Plant Pathol.* **95**: 155–162.
944
945

FIGURE AND TABLE CAPTIONS

Figure 1. Global Minimum Spanning Tree (MST). Displaying the relationships between STs at the triple-locus-variant level, illustrated using PHYLOViZ (Francisco *et al.*, 2012). The size of the circle correlates with the frequency of the ST. Color-coded accorded to origin: green = this study, black = PAMDB, blue = Visnovsky *et al.* (2016), purple = Japan.

Figure 2. Bayesian tree based on the concatenated alignment (2010 bp) of four housekeeping genes: *gapA*, *gyrB*, *gltA* and *rpoD*. The Bayesian tree was reconstructed using MrBayes based on the Tamura-Nei + G + I model using 30,000,000 MCMC. Single representative sequences for each ST were used to improve readability (corresponding STs and frequency of each ST listed in Table S2). Values indicated at nodes are Bayesian posterior probabilities. The corresponding phylogroups (PG) are indicated, eg. PG1 = phylogroup 1 with clades 1a and 1b. Origin of isolates is illustrated in colour coded boxes, green = this study, black = PAMDB, blue = Visnovsky *et al.* 2016, purple = Japan.

Figure 3. Global Bayesian tree reconstructed from *gltA* sequences highlighting the particularity of PG3a, which includes kiwifruit isolates from NZ, China, Japan, the US and France. The tree was built on a 529 bp alignment using MrBayes (TN+G+I model; 1,700,000 MCMC), using *Pseudomonas fluorescens* SBW25 as outgroup. Values indicated at nodes are Bayesian posterior probabilities. The source of each isolate is highlighted in colour-coded boxes, green = this study, red = China, black = PAMDB, purple = Japan, blue = US, NZ and France.

968
969 **Figure 4. Individual growth dynamics of *Psa* NZ54 and *P. syringae* G33C compared**
970 **with co-inoculation (1:1 ratio) *in vitro*.** Competition experiments were performed in
971 a 1:1 ratio (founding ratio $5x10^6$ cfu ml^{-1} each), with individual inoculations as
972 reference. Solid lines represent individual growth and dashed lines represent growth
973 in competition. The presented mean and standard error were calculated from three
974 replicates. Asterisk indicate significance between individual and co-cultured growth
975 at the 5% level (paired *t*-test).

976 **Figure 5. *In vitro* growth curves from invasion from rare experiments for *Psa* NZ54 :**
977 ***P. syringae* G33C and vice versa.** Vials were inoculated with a (A) 10:1 ratio and (B)
978 1:10 ratio for *Psa* NZ54 : *P. syringae* G33C. The presented mean and standard error
979 were calculated from three replicates. Parameters of relative fitness of *Psa* NZ54
980 relative to *P. syringae* G33C calculated as ln difference *Psa* NZ54 – *P. syringae* G33C
981 using the Malthusian parameters at 24hrs were -2.1* ±0.02 (KB shaken), -1.9*±0.05
982 (KB static), -12.1*±0.09 (M9 shaken) and -3.9*±0.00 (M9 static). Asterisks indicate
983 significance at the 1% level (Students *t*-test).

984 **Figure 6. 1:1 competition growth assays of *Psa* NZ54 vs. *P. syringae* G33C *in planta*.**
985 'Hort16A' plantlets (A) and 'SunGold' plantlets (B) were inoculated with a 1:1 mix of
986 *P. syringae* G33C : *Psa* NZ54 (founding density $8x10^7$ cfu ml^{-1}). (C) 'SunGold' plants
987 were inoculated with 1:1 mix of *P. syringae* G33C : *Psa* NZ13 Δ*hrcC* (founding density
988 $8x10^7$ cfu ml^{-1}). Solid lines represent individual growth and dashed lines represent
989 growth in competition. The presented mean and standard error were calculated
990 from the mean of four ('Hort16A') and five ('SunGold') individual measurements.

991 Asterisk indicate significance between individual and co-cultured growth at the 5%
992 level (paired *t*-test).

993 **Figure 7. Invasion from rare experiments for *Psa* NZ54 : *P. syringae* G33C *in planta*.**
994 'Hort16A' plantlets were inoculated with different ratios of strains *Psa* NZ54 : *P.*
995 *syringae* G33C. A) Individual growth. B) Invasion from rare 100:1 and C) invasion
996 from rare 1:100. Solid lines represent individual growth and dashed lines represent
997 growth in competition. The presented mean and standard error were calculated
998 from the mean of four individual measurements. Asterisks indicate significance
999 between individual and co-cultured growth at the 5% level (paired *t*-test).

1000 **Figure 8. *In planta* priority effect of *Psa* NZ54 or *P. syingae* G33C with subsequent**
1001 **inoculation of the respective second strain with the same founding density.** (A) *In*
1002 *planta* growth assay of *P. syringae* G33C using 'Hort16A' plantlets pre-inoculated for
1003 three days with *Psa* NZ54 ($8x10^7$ cfu ml^{-1}). (B) *in planta* growth assay of *Psa* NZ54
1004 using 'Hort16A' plantlets pre-inoculated for three days with *P. syringae* G33C ($8x10^7$
1005 cfu ml^{-1}). Solid lines represent individual growth and dashed lines represent growth
1006 in competition. The presented mean and standard error were calculated from the
1007 mean of five individual measurements. Asterisks indicate significance between
1008 individual and co-cultured growth at the 5% level (paired *t*-test).

1009 **TABLES**

1010 **Table 1: Nucleotide and amino acid diversity.** L = length in bp, AA = amino acid, GC =
1011 average GC content in %, N_A = number of alleles, P = number of polymorphic sites,

d_N/d_S ration, mut = mutations, π = nucleotide diversity indices, θ = Watterson's theta.

Table 2: Average pairwise genetic diversity between and among phylogroups. Analyses were conducted on the concatenated alignment (2006 bp, gaps removed) using the Maximum Composite Likelihood model with a gamma distribution of 1. N= number of strains.

Table 3: LDhat recombination analysis. Showing the length of the alignment in bp, N = number of sequences, mutation rate θ (=2Neμ) per site, recombination rate ρ (=2Ner) per site, ratio ε = ρ/ θ and Tajima's D.

SUPPORTING INFORMATION

Table S1. Geographic location of orchards, strain summaries and diversity indices per orchard. Specification of cultivar and infection status at the time according to KVH (Kiwifruit Vine Health), orchard ID, GPS coordinates, location and month of sampling, N = number of collected *P. syringae* strains, N PG3a = number of PG3a strains in total sample, N STs = number of unique STs, N STs PG3a = number of unique STs grouping with PG3a, D = Simpsons index of diversity, D_c = converted to effective number of species, ED = Simpsons evenness.

Table S2. List of all strains. Strain information and assigned sequence type of strains used for MLST study (all) and strains used for phylogenetic analysis (highlighted in grey). Phylogroup association only provided for isolates used for phylogenetic analysis. Alias provides the name used for competition experiments.

1033 **Table S3. PERMANOVA results of 3-factor nested analysis for differences in genetic**
1034 **diversity.**

1035 **Table S4. LDhat recombination analysis for host and disease status.** Length of
1036 alignment in bp, number of sequences, number of segregating sites, mutation rate θ,
1037 recombination rate ρ and ratio ε (ρ/ θ).

1038 **Table S5. LDhat recombination analysis for global data sorted according to**
1039 **phylogroup (PG).** Length of alignment in bp, N = number of sequences, number of
1040 segregating sites, mutation rate θ, recombination rate ρ and ratio ε (ρ/ θ).

1041 **Table S6. List of primers used for construction of the deletion mutant *Psa* NZ13**
1042 **Δ*hrcC*.**

1043 **Figure S1. Rarefaction curves based on the concatenated sequences.** Two curves
1044 each are shown for *P. syringae* (n=148) and the sequences grouped according to
1045 phylogroups (PG): solid lines represent grouping based on unique STs and dashed
1046 lines according to a cut-off equal to the average pairwise genetic distance of the
1047 group: PG1, PG2 & PG3 = 0.02 cut-off, Psyr all = 0.05 cut-off.

1048 **Figure S2. Shared and unique STs among orchards.** Gold I = infected 'Hort16A'; Gold
1049 NI= uninfected 'Hort16A'; Green NI = uninfected 'Hayward'; Green I = infected
1050 'Hayward' orchard; n= number of STs found in orchard.

1051 **Figure S3. eBurst snapshot of STs at the single locus variant level.** The size of the
1052 circles correlates with the frequency of the respective ST found in the dataset.
1053 Colours correspond to the different orchards, orange = infected 'Hort16A', yellow =

uninfected 'Hort16A, dark green = infected 'Hayward', light green = uninfected 'Hayward'. CC = clonal complex.

Figure S4. Maximum Likelihood trees based on single genes. Each Maximum Likelihood tree is rooted on *Pseudomonas fluorescens* SBW 25 and was reconstructed using TREEPUZZLE based on the Tamura-Nei model using 100,000 puzzling steps. Trees were built using single representatives of each unique ST to improve readability of the tree. Values indicated at nodes are bootstrap values. The corresponding phylogroup distinctions based on the concatenated ML tree are indicated with the coloured squares.

Figure S5. Leaves of 'Hort16A' plants inoculated with *Psa* NZ54, *P. syringae* G33C and a 1:1 mix of *Psa* NZ54 : *P. syringae* G33C at 2, 4, and 7 days post inoculation.

Figure S6. Leaves of 'SunGold' plants inoculated with *Psa* NZ54, *P. syringae* G33C, *Psa* NZ13 ΔhrcC and 1:1 mix of the respective strain combinations at 3 and 7 days post inoculation. For leaves showing minor leaf spots, the lower side of the leaf is also shown for easier detection of symptoms.

Figure S7. *In planta* priority effect of *Psa* NZ54 or *P. syringae* G33C with subsequent inoculation of the second strain with 100-fold lower concentration. *In planta* growth assay using 'Hort16A' plantlets pre-inoculated ($8x10^7$ cfu ml^{-1}) with one strain followed by inoculation of the second strain at ($8x10^5$ cfu ml^{-1}). The two panels display growth curves for endo- and epiphytic growth respectively. A) Individual growth, B) inoculation of *Psa* NZ 54 at day 3 and C) inoculation of *P. syringae* G33C at 3 dpi. Solid lines represent individual growth and dashed lines represent growth in

competition. The presented mean and standard error were calculated from the mean of five individual measurements. Asterisks indicate significance between individual and co-cultured growth at the 5% level (paired *t*-test).

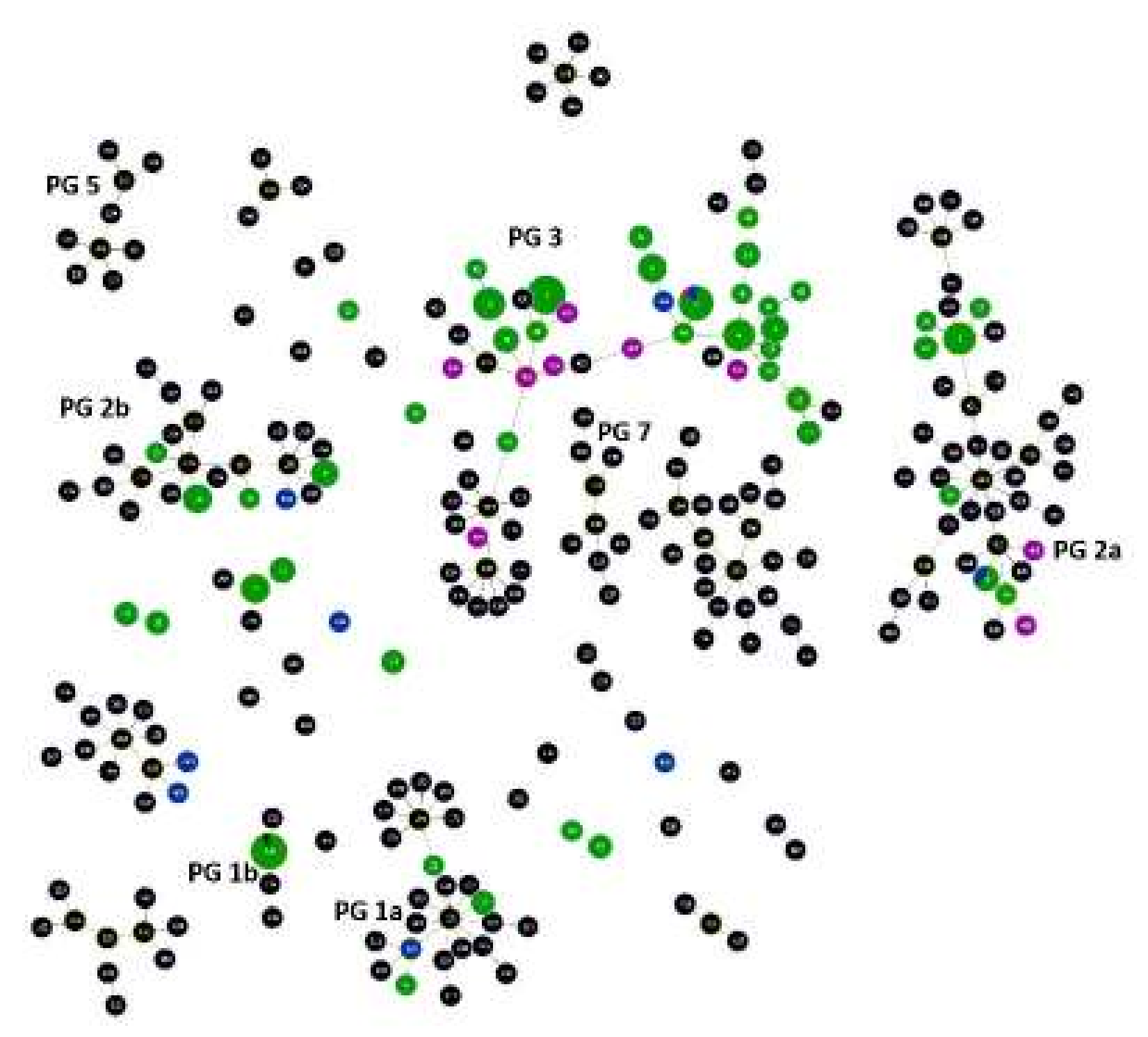
PG 5
PG 3
PG 2b
PG 7
PG 2a
PG 1b
PG 1a

KW17–1
G23B–I
KW1–1
H24C–I
R15B–I
H34A–I
H25C–II
H24B–I
R33B–II
R33B–I
R34A–I
K14C–I
H23B–I
R16C–I
KW2–1
KW22–2
KW22–1
P. syringae ICMP19499
H33A–I
R26A–I
G22C–I
KW8–1
R25B–II
H31A–I
K35C–I
R35A–I
R11B–III
KW23
H12B–I

PG3a

PG3

P. syringae pv. *phaseolicola* KN86
P. syringae pv. *phaseolicola* 1448A
P. syringae pv. *glycinea* BR1
P. syringae pv. *savastanoi* LMG 2209 BS2738
P. syringae pv. *mori* M301020
P. syringae pv. *mellea* N6801
P. syringae pv. *tabaci* 6606
P. syringae pv. *lachrymans* N7512
P. syringae pv. *morsprunorum* FTRS_U7
P. syringae pv. *myricae* AZ84488
P. syringae pv. *pisi* H5E3
P. syringae pv. *japonica* M301072
P. syringae pv. *atrofaciens* LMG 5095 BS2457
H36C–I
K11A–II
P. syringae pv. *syringae* LOB2_1
P. syringae pv. *aptata* 601
G16C–II
P. syringae ICMP11168
K16A–II
P. syringae pv. *pisi* NCPPB 2585 BS2753
H31B–I
G31A–II
G32B–I
G25A–I
G31C–II
G14C–X
G31A–I
P. syringae ICMP13102
P. syringae pv. *syringae* PD2774
G24B–I
P. syringae pv. *papulans* LMG 5076 BS2752
H25B–II
H25B–I
G34C–II
P. syringae Cit7
KW22–3
G35B–I
G21C–II
KW8–2
R31A–II
P.syringae pv. *broussonetiae* KOZ8101
P. syringae pv. *tagetis* LMG 5090 BS2754
P. syringae pv. *helianthi* LMG 5067 BS2749
H16B–I
G16C–I
P. syringae pv. *syringae* PD2766
P. syringae pv. *coriandricola* BS2705
P. syringae pv. *cilantro* 0788_9
P. syringae pv. *oryzae* I_6
P. syringae pv. *coronafaciens* KN221
P. syringae pv. *oryzae* 36_1
P. syringae pv. *syringae* Ps9220
P. syringae ICMP11292
G36B–I
P. syringae pv. *apii* LMG 2132 BS2456
P. syringae pv. *maculicola* 4981
H35B–I
G16B–I
P. syringae pv. *maculicola* M2 pathotype
P. syringae pv. *maculicola* KN84
P. syringae pv. *tomato* DC3000
P. syringae pv. *actinidiae* FTRS_L1
G13A–I
P. syringae pv. *thea* K93001
P. syringae pv. *actinidiae* biovar 4 ICMP19497
P. syringae pv. *ribicola* LMG 2276 BS2741
P. syringae pv. *primulae* LMG 2252 BS2740
P. fluorescens SBW25

PG2
PG6
PG5
PG4
PG1
PG7
1a
1b

0.01

Japan NZ PAMDB Visnovsky *et al.* 2016

PG3a

PG3

PG2

PG4

PG6

1a

PG1

1b

PG5

PG7

R25B–II
H31A–I
91L6
R34A–I
R33B–II
R33B–I
K35C–I
K14C–I
H23B–I
R26A–I
G22C–I
50S1
KW23
KW17–1
G23B–I
50S3
47L9
R35A–I
R15B–I
R11B–III
H12B–I
R16C–I
H34A–I
H33A–I
H24B–I
KW22–2
KW22–1
H25C–II
H24C–I
91L4
KW8–1
KW2–1
KW1–1
171L9
171L1
P. syringae ICMP19499
122L1
P. syringae pv. *savastanoi* PT LMG 2209 BS2738
P. syringae pv. *morsprunorum* FTRS_U7
91L2
84L8
228L2
25S10
P. syringae pv. *tabaci* 6606
P. syringae pv. *lachrymans* N7512
P. syringae pv. *myricae* AZ84488
P. syringae pv. *mori* M301020
P. syringae pv. *mellea* N6801
P. syringae pv. *phaseolicola* 1448A
P. syringae pv. *phaseolicola* KN86
P. syringae pv. *glycinea* BR1
82L1
P. syringae Cit7
174L8
2L2
KW8–2
KW22–3
G35B–I
G21C–II
P. syringae pv. *papulans* PT LMG 5076 BS2752
G24B–I
53L5
R31A–II
P.syringae pv. *broussonetiae* KOZ8101
H25B–II
H25B–I
G34C–II
P. syringae pv. *aptata* 601
P. syringae pv. *syringae* LOB2_1
K16A–II
P. syringae ICMP11168
H36C–I
P. syringae pv. *japonica* M301072
P. syringae pv. *atrofaciens* PT LMG 5095 BS2457
K11A–II
P. syringae pv. pisi H5E3
G16C–II
G25A–I
G32B–I
G14C–X
G31C–II
G31A–II
P. syringae pv. *pisi* PT NCPPB 2585 BS2753
H31B–I
G31A–I
P. syringae ICMP13102
P. syringae pv. *syringae* PD2774
P. syringae pv. *syringae* Ps9220
P. syringae pv. *oryzae* I_6
P. syringae pv. *coronafaciens* KN221
P. syringae pv. *oryzae* 36_1
P. syringae pv. *tagetis* PT LMG 5090 BS2754
P. syringae pv. *helianthi* PT LMG 5067 BS2749
P. syringae pv. *tomato* DC3000
P. syringae pv. *maculicola* M2 pathotype
P. syringae pv. *maculicola* KN84
P. syringae pv. *maculicola* 4981
G16B–I
P. syringae ICMP11292
G36B–I
H35B–I
P. syringae pv. *apii* PT LMG 2132 BS2456
50L1
P. syringae pv. *actinidiae* FTRS_L1
G13A–I
P. syringae pv. *thea* K93001
P. syringae pv. *actinidiae* biovar 4 ICMP19497
65L3
P. syringae pv. *coriandricola* BS2705
P. syringae pv. *cilantro* 0788_9
89P1
206L2
206L8
P. syringae pv. *ribicola* PT LMG 2276 BS2741
75L9
P. syringae pv. *primulae* LMG 2252 BS2740
47L1
H16B–I
G16C–I
P. syringae pv. *syringae* PD2766
P. fluorescens SBW25

0.008

China
NZ
Visnovsky *et al.* 2016
Japan
PAMDB

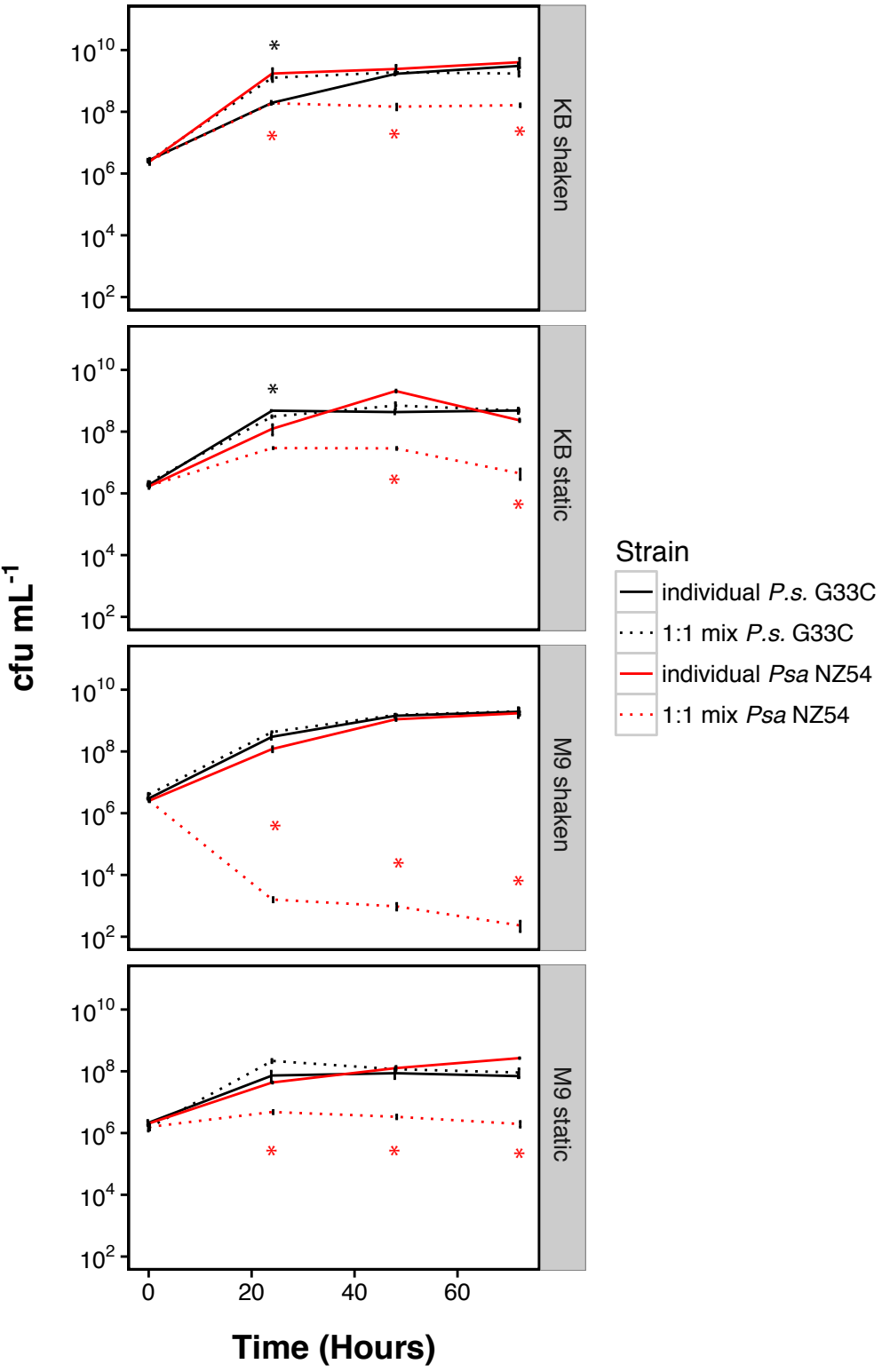
KB shaken
KB static
M9 shaken
M9 static
cfu mL-1
Time (Hours)
0
20
40
60
Strain
individual P.s. G33C
1:1 mix P.s. G33C
individual Psa NZ54
1:1 mix Psa NZ54

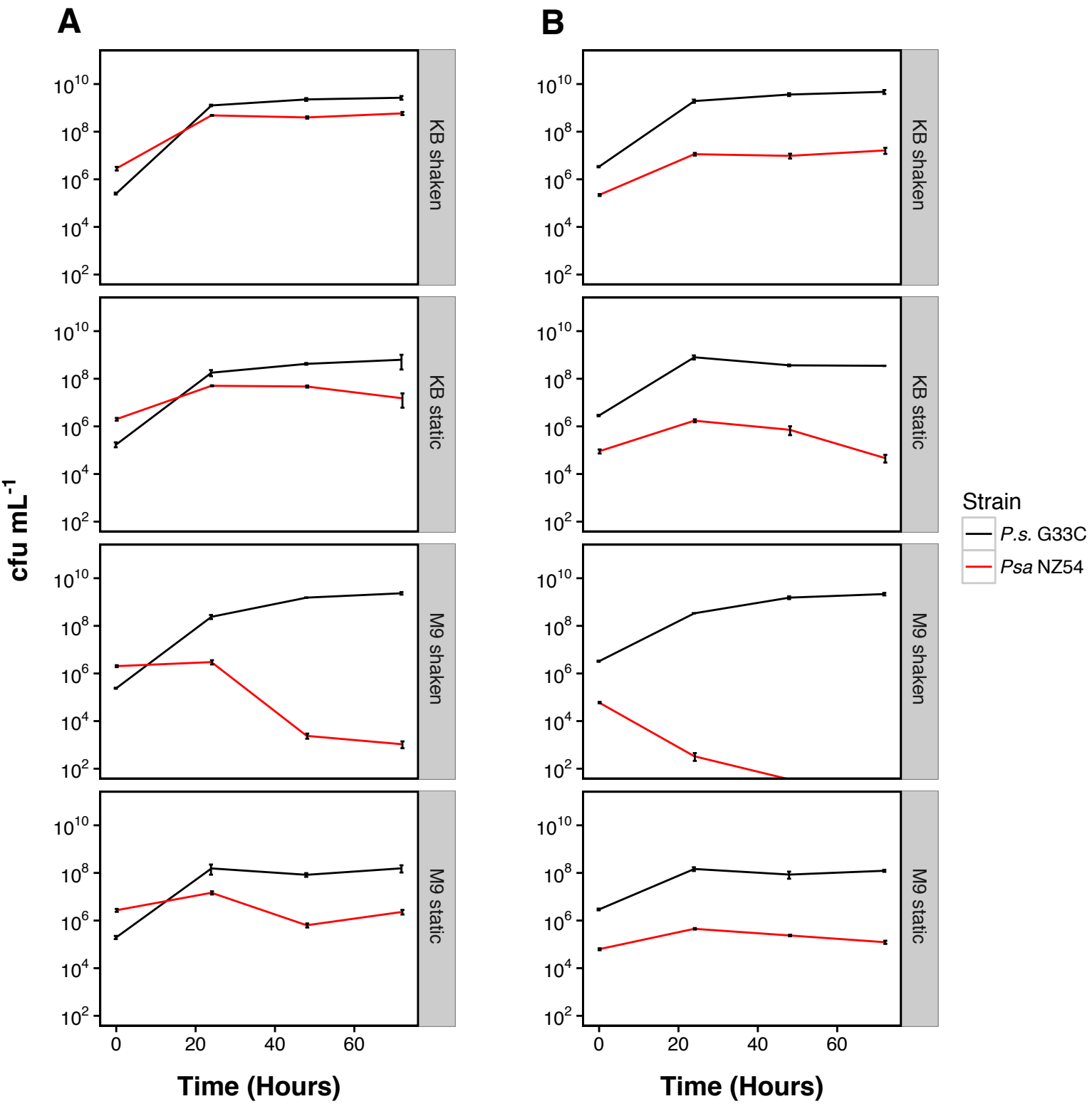
A
B
KB shaken
KB static
M9 shaken
M9 static
cfu mL-1
Time (Hours)
Strain
P.s. G33C
Psa NZ54

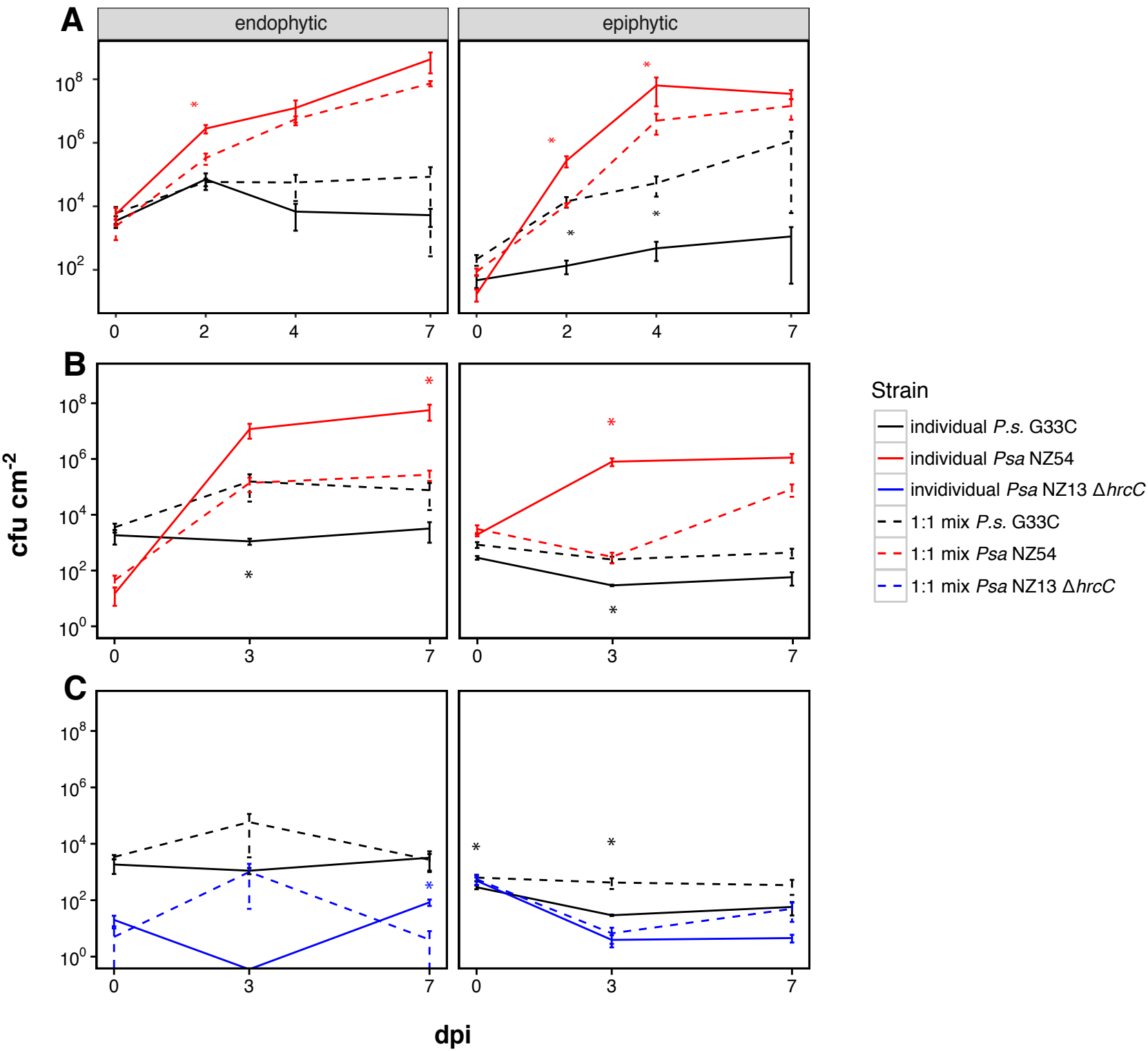
A
endophytic
epiphytic
B
C
cfu cm-2
dpi
Strain
individual P.s. G33C
individual Psa NZ54
invidividual Psa NZ13 ΔhrcC
1:1 mix P.s. G33C
1:1 mix Psa NZ54
1:1 mix Psa NZ13 ΔhrcC

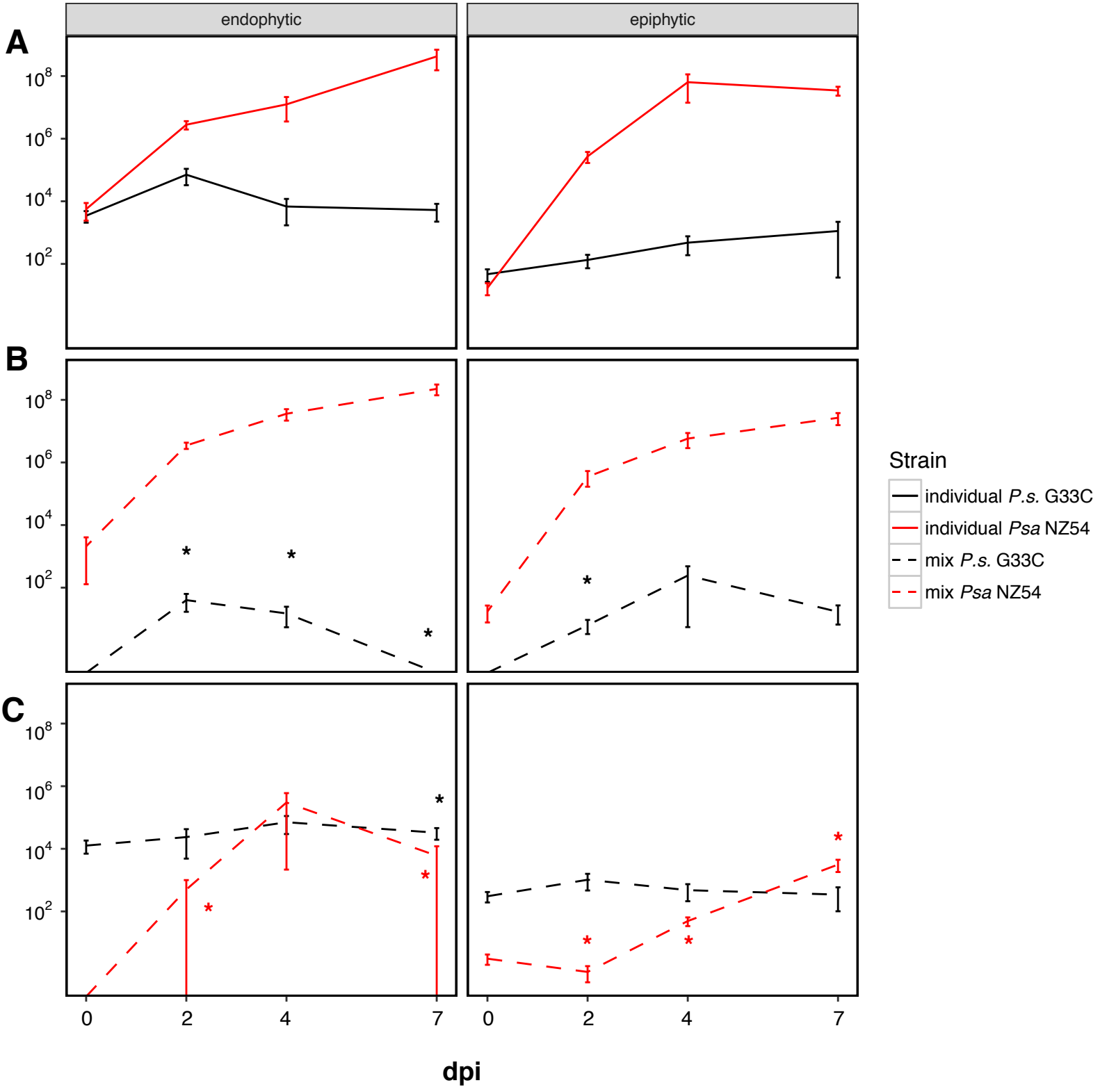
endophytic
epiphytic
A
B
C
10^8
10^6
10^4
10^2
0
2
4
7
dpi
Strain
individual *P.s.* G33C
individual *Psa* NZ54
mix *P.s.* G33C
mix *Psa* NZ54

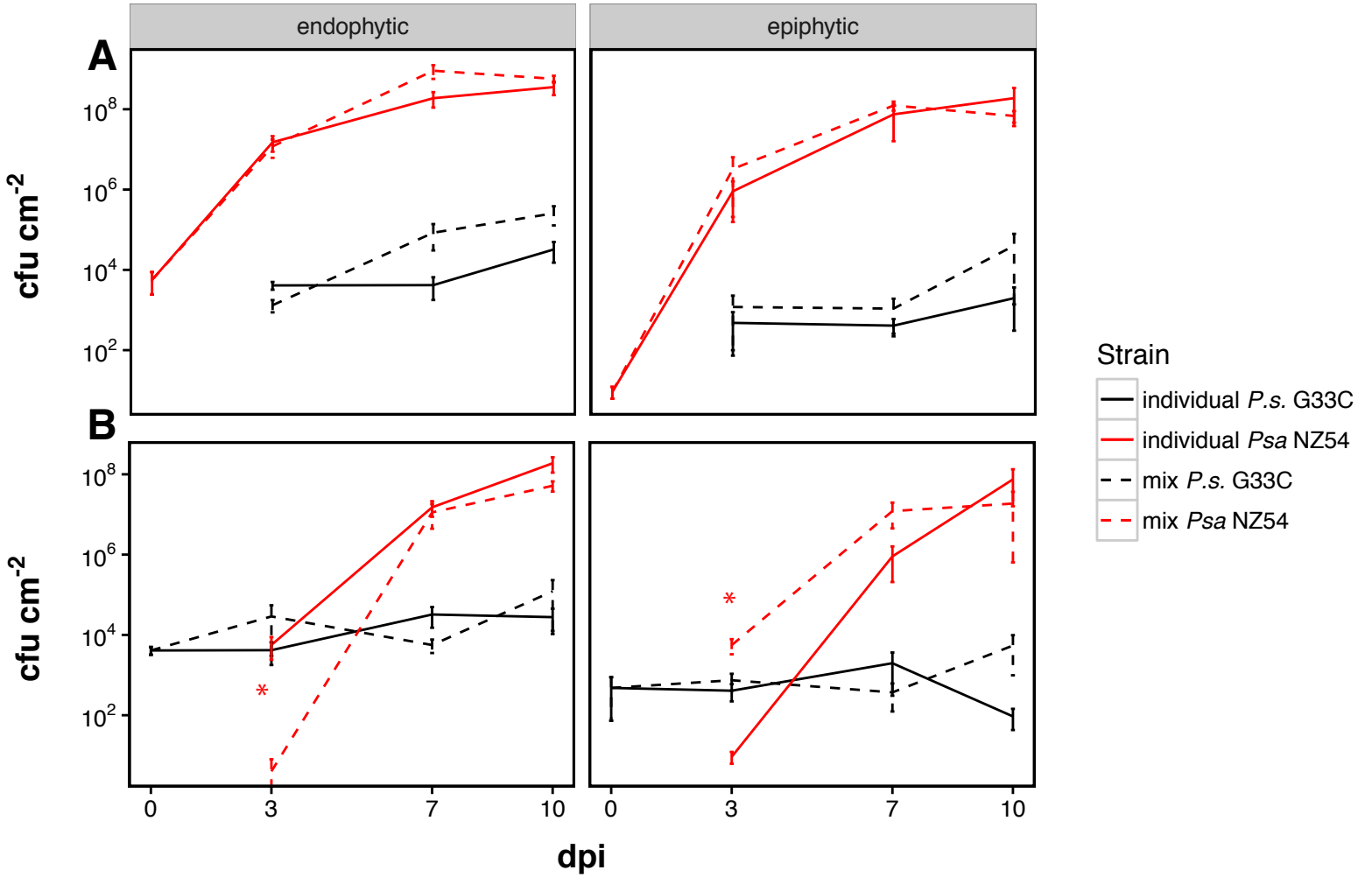
endophytic
epiphytic
A
B
cfu cm-2
10^8
10^6
10^4
10^2
*
0
3
7
10
dpi
Strain
individual P.s. G33C
individual Psa NZ54
mix P.s. G33C
mix Psa NZ54

Table 1. Nucleotide and amino acid diversity. L = length in bp, AA = amino acid, GC = average GC content in %, N_A = number of alleles, P = number of polymorphic sites, d_N/d_S ration, mut = mutations, π = nucleotide diversity indices, θ = Watterson's theta.

Locus	L (bp)	AA length	GC	N_A	P*	d_N/d_S	mut	π	θ
gapA	476	158	60.81	25	80 (16.81)	3.365	97	0.055	0.024
gyrB	507	169	53.15	28	145 (28.60)	0.018	184	0.054	0.041
gltA	529	176	58.45	27	88 (16.64)	0.011	102	0.040	0.025
rpoD	495	166	59.56	35	99 (20)	2.022	118	0.042	0.030
Mean	502	167	57.99	29	105 (20.51)	1.354	125	0.048	0.030

Table 2. Average pairwise genetic diversity between and among phylogroups. Analyses were conducted on the concatenated alignment (2006 bp, gaps removed) using the Maximum Composite Likelihood model with a gamma distribution of 1. N= number of strains.

N	Phylogroup	1	2	5	3
19	**1**	0.010			
43	**2**	0.098	0.027		
3	**5**	0.111	0.106	0.008	
83	**3**	0.099	0.063	0.107	0.014

Table 3. LDhat recombination analysis. Showing the length of the alignment in bp, N = number of sequences, mutation rate θ (=2Neμ) per site, recombination rate ρ (=2Ner) per site, ratio ε = ρ/ θ and Tajima's D.

Gene	Length (bp)	N	Segregating sites	θ	ρ	ε = ρ/θ	Tajima's *D*
All *P. syringae*:							
concatenated	2010	148	335	0.030	0.006	0.187	0.513
gapA	476	148	63	0.024	0.021	0.902	2.204
gyrB	507	148	116	0.041	0.038	0.931	-0.204
gltA	529	148	74	0.025	0.012	0.461	0.678
rpoD	498	148	82	0.030	0.012	0.416	0.03
Phylogroup 1							
concat	2010	19	66	0.009	0.000	0.000	0.207
gapA	476	19	8	0.005	0.000	0.000	0.407
gyrB	507	19	20	0.011	0.000	0.000	0.611
gltA	529	19	19	0.010	0.000	0.000	0.026
rpoD	498	19	19	0.011	0.000	0.000	-0.188
Phylogroup 2							
concat	2010	43	147	0.017	0.002	0.120	1.754
gapA	476	43	29	0.014	0.006	0.457	2.307
gyrB	507	43	63	0.029	0.000	0.000	2.131
gltA	529	43	27	0.012	0.008	0.654	0.993
rpoD	498	43	28	0.013	0.023	1.734	0.621
Phylogroup 3							
concat	2010	83	163	0.016	0.015	0.937	-0.746
gapA	476	83	34	0.014	0.013	0.898	2.096
gyrB	507	83	96	0.038	0.024	0.636	-2.434
gltA	529	83	13	0.005	0.006	1.175	1.991
rpoD	498	83	20	0.008	0.033	4.073	0.3
Phylogroup 5							
concat	2010	3	23	0.008	0.000	0.000	-
gapA	476	3	-	-	-	-	-
gyrB	507	3	13	0.017	0.000	0.000	-
gltA	529	3	3	0.004	0.000	0.000	-
rpoD	498	3	7	0.009	0.000	0.000	-